## ABSTRACT

Mechanical patterns on cell culture substrates can be potentially used as effective cues in directing cell migrations. Fully functional substrates require not only readily tunable modulus to generate mechanical stimuli but also proper surface properties to ensure proper interactions with the surrounding media.

In this study, crosslinked polydimethylsiloxane (PDMS) with tunable modulus ranging from 50 to 1000 kPa was fabricated using platinum-catalyzed hydrosilylation between vinyl and -SiH functionalized PDMS pre-polymers. Substrate modulus was tuned as a function of the density of the reactive moieties (-SiH) on crosslinkers, the molar ratio between vinyl and -SiH functionalities, and the average molecular weight between adjacent crosslinkers.

To overcome the hydrophobicity of PDMS surfaces, mono-vinyl-terminated polyethylene glycol (V-PEG) was grafted onto crosslinked PDMS thin films containing excess -SiH functionality via surface hydrosilylation reaction. Efficiency of surface PEGylation was controlled by surface density of -SiH groups, molecular weight of V-PEG, and catalyst concentrations.

# PREPARATION AND SURFACE PEGYLATION OF CROSSLINKED POLYDIMETHYLSILOXANE SUBSTRATES WITH TUNABLE MODULI

WANXIN WANG

Thesis advisor: Wei Chen

A thesis presented to the faculty of Mount Holyoke College in partial fulfillment of the requirements for the degree of Bachelor of Arts with honors

May 2013

Chemistry Department

## ACKNOWLEDGEMENTS

First, I would like to acknowledge my advisor, Prof. Wei Chen, for her inspiration, guidance, and unconditional support. She led me into the exciting field of biomaterials where I discovered my research passion, and fostered my research capacity with pertinent advice and trust. Her persistence, enthusiasm, and creativity for research instilled faith in my pursuit as a scientist and engineer.

I would also like to thank Prof. Maria Gomez and Prof. Katherine Aidala, for the generous insights they provided as my committee members and the immense impact they made on my undergraduate study as my academic mentors.

I want to acknowledge Prof. Lilian Hsu, for introducing me into the world of scientific research, and helping me with incessant suggestions and encouragement.

I acknowledge my project mentor Mojun Zhu. She inspired me to continuously thrive for my dreams. I thank my fellow labmates in Wei's group: Lanhe Zhang, Mimi Hang, Yen Nguyen, Lien Nguyen, and Ye Tian, for questions, discussions, and good humor.

I would like to dedicate this thesis to my parents, who give me courage with their unconditional love and understanding, and to my friends Xintong Zuo, Yiwen Liu, and Haibei Peng, who shared the most wonderful four years of undergraduate life with me.

## CONTENTS

## LIST OF FIGURES AND TABLES

# 1. INTRODUCTION

## 1.1 Inspiration for this Project

*Directional cell migrations and mechanotaxis.* Development and maintenance of multicellular organisms require orchestrated movement of cells in designated directions. While intracellular cytoskeletal elements and their dynamic polymerization and depolymerization provide molecular basis for the movement of cells, extracellular stimuli polarize migrating cells and bias their movements into particular directions.

Extracellular matrix (ECM) is the direct milieu of migrating cells. It is the reservoir of biochemical and biomechanical cues that orient cells' movement.[1] Migration control by gradients of dissolved or surface-adhered chemoattractants (chemotaxis and haptotaxis, respectively) has been studied extensively since 1965.[2-4] It was not until 2000, however, did Lo *et al.* identify that gradient of stiffness in ECM was also capable of guiding cell migrations.[5] The discovery established the concept of mechanotaxis, the directional movement of cells in response to the gradient of ECM stiffness.

Mechanotaxis was first observed on a mechanical gradient established by juxtaposed hard and soft hydrogels as directional cellular movement towards the harder domain.[6] While migration up the mechanical gradients has since been commonly observed among various cell types,[6,7] the exact mechanism that associates the mechanical signals and intracellular responses remains largely unknown. Therefore, how purely physical interactions at the cell-substrate

interface dictates cell migrations has generated research interests in mechanobiology. One major challenge for the study, however, is to mimic the stiffness gradient *in vitro* with appropriate substrate design. The challenge proves to be twofold. First of all, systematic preparation of substrates with precisely characterized mechanical properties and defined geometries of soft and hard domains has not yet been realized due to technical difficulties.[8-18] Secondly, surface chemistry of substrate materials should be readily tailored to prevent non-specific protein adsorption and provide appropriate binding epitopes for transmembrane cytoskeletal elements.[19] The goal is to create a biochemical environment comparable to ECM to support cell survival, adhesion, and migration.

Although the biological aspects of mechanotaxis have been widely investigated, more efforts must be focused on better defining and controlling the mechanical stimulus so that it can be reliably correlated with cell migratory behaviors. This project was therefore initiated as an attempt to develop a substrate system with tunable mechanical properties and proper surface chemistry to study mechanotaxis.

## 1.2 Polymeric Biomaterials

Biomaterials are materials intended to interface with biological systems to evaluate, treat, augment, or replace any tissue, organ, or function of the body.[20] For the study of mechanotaxis, polymeric biomaterials or biopolymers are the most commonly employed substrate materials. This can be attributed to the

inherent flexibility in synthesizing or modifying polymers so that the physical and mechanical properties of ECM can be readily emulated.

The most common biopolymer scaffolds used in studying mechanotaxis are collagen or collagen-derived scaffolds prepared as soft hydrated gels, which represent a group of naturally-occuring biopolymers including elastin and polysaccharide nanofibers. The advantage of this group of biomaterials is obvious: as major ECM components, they are less likely to evoke inadvertent immune response on one hand, and on the other hand, they are able to provide binding motif for cell attachment without further chemical modifications. Their drawback, however, the swelling characteristics inherent in hydrogels in aqueous solutions, proves to be equally apparent for our purpose. Specifically, swelling of a crosslinked polymer network is characterized as an increase in substrate volume by absorbing large amount of solvent. Differential swelling will occur at substrate domains with different crosslink densities, leading to an uneven surface topography. Therefore, nanoscale surface topography is inevitable in hydrogel system since crosslink density is a major parameter to be manipulated in order to obtain different substrate stiffness. However, it has been shown that surface topography influences cell migration behaviors[21] and will therefore complicate our study.

The concern for the swelling behavior of substrate materials eliminate the candidacy of naturally occurring biopolymers mentioned above as well as other hydrogel-based polymers such as polyacrylamide, which is another widely used

material system. Among non-hydrated synthetic polymers, carbon fibers are not ideal due non-biodegradability. In this project, siloxane polymers were chosen as the substrate material because its unique combination of properties, including hydrophobicity and readily controllable degree of crosslinking and surface chemistry, serves our purpose.

### 1.3 Polydimethylsiloxane: From Structure to Properties

In this project, polydimethylsiloxane (PDMS) was chosen as the substrate material due to its desirable properties. Most of them are closely related to the chemical structure of the siloxane polymer.

The electronegativity of silicon is not only lower than oxygen, but also lower than carbon and hydrogen. The relatively large gap in electronegativity between oxygen (3.5) and silicon (1.9) renders 51% ionic character to the Si-O bond,[22] which sets siloxane polymers apart from carbon-based polymers. Thermodynamically, the Si-O bond is stronger (110 kcal/mol) than the C-C bond (83 kcal/mol), giving PDMS better thermal stability than hydrocarbon polymers. In addition, lacking functional groups and with the highest oxidation state of silicon, PDMS is inert to most chemical reagent (except for acid and base) and oxidation.

The chemical structure of PDMS is shown in Figure 1. The Si−O and Si−C bond lengths (1.63 and 1.90 Å) have been reported to be over 7% longer than the C−C bonds (1.53 Å) in carbon-based polymers. The Si−O−Si bond angle (143°) is not only much greater than the C−C−C bond angles (109.5°) but can

also readily pass through 180°. These differences, along with the partial ionic nature of Si−O bonds, allow pairs of methyl group to rotate around the Si−O alternating backbone and permit dimethyl groups to swing around the silicon atoms they are bound to. The free rotation and swing of the methyl groups gives PDMS both torsional and bending flexibility, leading to the low glass transition temperature of PDMS (−125 °C). Meanwhile, the hydrophobic nature of methyl groups contributes to the non-swelling characteristics of PDMS so that it can be used in water and alcohol solvents without noticeable material deformation. The motility and hydrophobicity of the methyl groups renders PDMS surfaces highly hydrophobic.

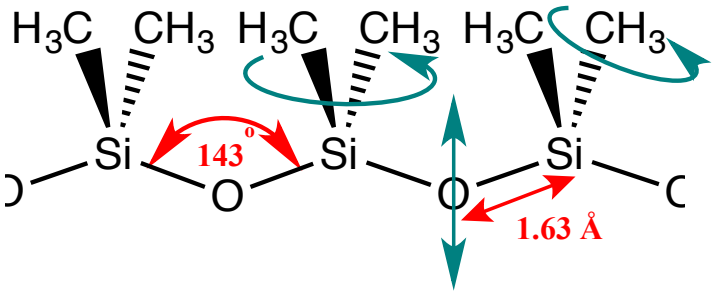


**Figure 1.** Chemical structure of polydimethylsiloxane with depictions of motions of methyl groups.

The biocompatibility of PDMS in a variety of forms has been well recognized through its clinical applications, including breast prostheses, artificial skins, contact lenses, etc. Possible toxicity that may result from chemical impurities such as catalysts used in polymerization reactions has been investigated. Their identities, threshold levels, and possible ways of elimination have been profiled in details.[23] Moreover, PDMS is biodegradable due to its

amenability to a series of degradation reactions,[24] which makes it superior as biomaterials over hydrocarbon-based materials.

To this end, the characteristics of PDMS can be summarized as: thermally stable, chemically inert, non-swelling in aqueous solutions, biocompatible, biodegradable, and low in surface tension. Of all these properties, the first five make PDMS a highly desirable candidate material for our purpose. The last property, that is, the hydrophobic nature of PDMS surfaces, imparts possibilities of non-specific protein adsorptions and subsequent immunogenic reactions as PDMS interfaces with cells. Therefore in this project, overcoming the hydrophobic nature of PDMS surfaces is one major aspect of investigation.

### 1.4 Crosslinking of PDMS

A *crosslink* is a bond that links one polymer chain to another. Covalent chemical bonds are one major form of crosslinks.[25] Their presence and density have a profound influence on the mechanical properties of materials. Without crosslinks, macromolecules exist as entangled chains that can easily disentangle and flow through each other (Fig. 2(a)). As a result, uncrosslinked polymers generally melt or flow as heat or mechanical stress is applied.

In contrast, crosslinked polymers cannot melt or flow freely because of the constraints on molecular motion introduced by the crosslinks (Fig. 2(b)). No permanent deformation occurs upon stress or strain, rendering crosslinked polymers elastic property. These polymers are called elastomers, as they are polymers with elastic properties.


**Figure 2.** Structural illustrations of (a) uncrosslinked and (b) crosslinked polymer networks.

Uncrosslinked PDMS is liquid at room temperature with a glass transition temperature of -125 °C. The crosslinking of PDMS to form elastomers was first realized in the 1940s[26, 27, 28] via bimolecular radical coupling between methyl groups. The method was soon improved by replacing terminal methyl groups with vinyl groups, which reduces the amount of radical initiators required, and was further advanced with the discovery of platinum-catalyzed hydrosilylations. Hydrosilylation proceeds as Si-H bond adds across unsaturated bonds. The reaction itself is not spontaneous thermodynamically but can be initiated by free-radical initiators, nucleophilic-electrophilic catalysts, and transition metal salts and complexes. Since its discovery in 1972, hydrosilylation has been one of the most fundamental methods for the laboratory and industrial synthesis of organosilicon and silicon related compounds.[29]

With the continual development in the efficiency of platinum-based catalysts,[30] hydrosilylation of hydrosilanes and olefins catalyzed by platinum complexes becomes one of the most widely used approaches to form silicon-carbon bonds. The general mechanism of hydrosilylation has been extensively

investigated and was proposed in Figure 3 by Lewis.[31] Specifically, as reported by a number of groups, oxygen plays an interesting role in the reaction in that it is required in the induction phase of the reaction whereas it disrupts multinuclear platinum species via conjugation when poorly stabilizing olefins are used.

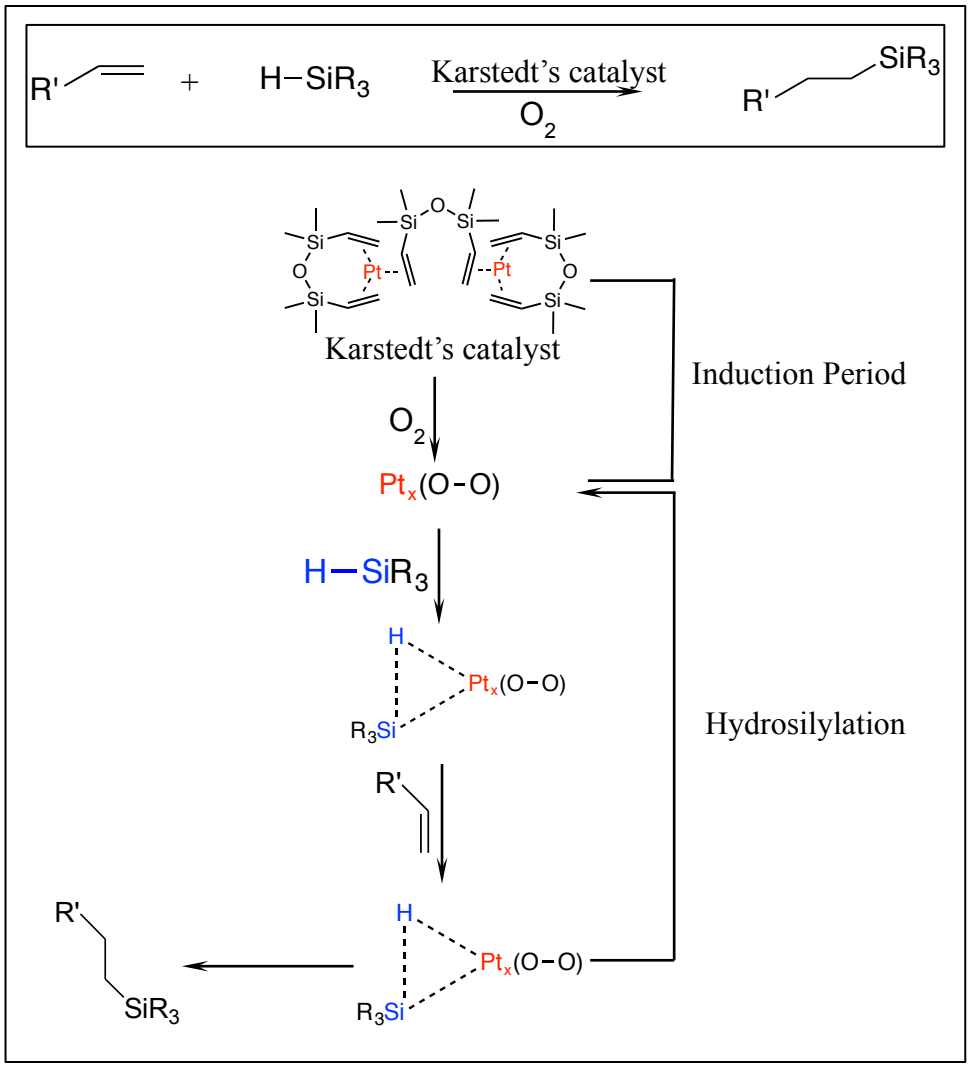


**Figure 3.** Proposed mechanism of hydrosilylation initiated by Karstedt's catalyst.

So far, almost all published studies that utilize platinum-catalyzed hydrosilylation to fabricate crosslinked PDMS use Sylgard 184, a Dow Corning

product. The moduli of the resulting substrates are therefore largely limited by the formulation of the commercial kit, and the surface chemistry is complicated by the presence of silica additives (~50 wt%) and other hydrophobic low molecular weight species (~5 %). Therefore, a simplified and better-controlled formulation system is proposed by this study.

### 1.5 Mechanical Characterization: Tensile Test

Along with compressive test and nanoindentation, tensile test is one of the most commonly employed mechanical tests of elastomers for determining mechanical properties such as Young's (elastic) modulus, yield strength, and yield point. A typical tensile stress over tensile strain curve generated via tensile test of a polymeric material is shown below (Figure 4). Specifically, the point at which the curve starts to behave nonlinearly is called the proportionality limit (A), where the elastic behavior of the material ends; the local maximum (B) is called the yield point, indicating the onset of plastic (i.e. permanent) deformation. Beyond the yield point, the material stretches considerably and forms the plastic "neck". Further elongation leads to an abrupt increase in stress (i.e. strain hardening) and the ultimate rupture of the material (C). Therefore, the linear domain of the tensile curve is used to characterize the elastic characteristics of the crosslinked PDMS monoliths in this project.

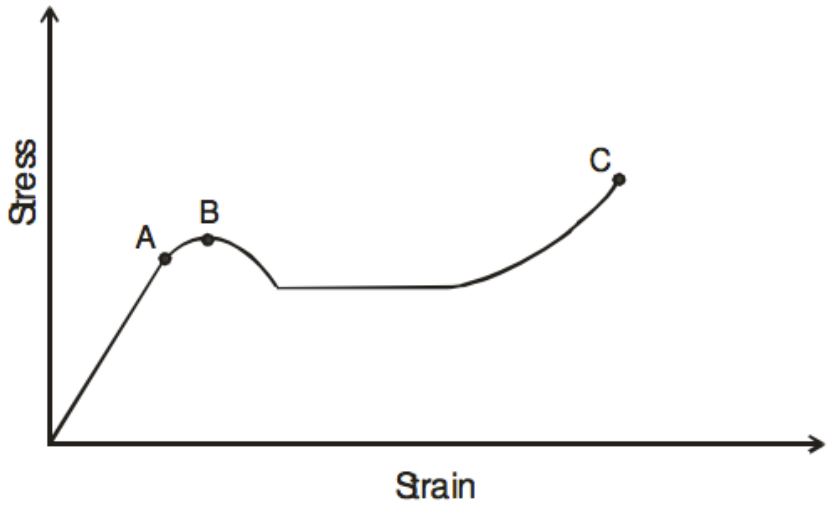


**Figure 4.** A typical tensile stress over tensile strain curve of a polymeric polymer.[32]

While the characteristic stress-strain curve of an elastomer is obviously dependent on molecular and structural parameters of the material, it is also affected by extrinsic factors such as the strain rate and temperature. It is sometime difficult to give a clear distinction between the elastic strain and permanent strain, because the extent to which a polymer can recover its original dimension depends on both temperature and the time allowed for recovery to occur.[33] Therefore, correct interpretation of the stress-strain curve to describe the elastic property of the material requires proper selection of the two parameters. American Society for Testing and Materials (ASTM) recommends an average strain rate of 0.5 cm/min.

### 1.6 Surface Modification of Crosslinked PDMS Thin Films

As discussed in section 1.3, highly flexible Si−O backbone and hydrophobic methyl groups give rise to the low surface tension of uncrosslinked PDMS ($\gamma$~20 dyn/cm). Crosslinked PDMS networks conserve most of the

properties of linear PDMS fluids, such as thermal stability, chemical inertness, and low surface energy. Despite the many merits of crosslinked PDMS inherent in its bulk properties, the hydrophobic nature of PDMS surfaces is problematic in our study. To begin with, introducing aqueous solutions into the substrate system will be difficult. Water, however, is known as one of the major constituents of ECM to ensure proper functionalities.[34] Moreover, PDMS-based cell migrating substrates are designed to directly interface with cells and their culturing media, both of which provide various types of proteins. Hydrophobic PDMS surfaces will facilitate non-specific adsorption of these proteins via hydrophobic interactions, leading to undesired consequences in multiple concerns. First of all, randomly deposited proteins may unpredictably change the substrates' mechanical properties, which deviates the mechanical stimulus from its original design and makes it inconsistent from time to time. Secondly, conformations of membrane-bound proteins dictate cell adhesion, survival, and migration. Non-specific protein adsorption may trigger conformational change and therefore denaturation of functional proteins. Furthermore, non-specific protein adsorption is known as the first step of foreign body reactions, leading to immunogenic responses and device failures.[35] Therefore, surface modification is necessary in order to overcome the hydrophobicity of crosslinked PDMS and to construct functional cell migration substrates.

Many methods have been developed to overcome the hydrophobic nature of PDMS surfaces. Although numerous ways of classifications are presented in

literatures based on different considerations, these methods can be loosely divided into two categories: 1) *physical oxidation*, including plasma treatment, UV/ozone treatment, and electrical discharge, etc.;

2) *chemical modifications,* including hydrosilylation, silanization, sol-gel coating, etc. Among methods of physical oxidation, oxygen-plasma treatment is most widely employed due to its convenience and low cost. However, the method is also known with its relative aggressiveness and rapid hydrophobic reconstruction after the treatment.[36] Silanization and hydrosilylation are two major reactions used in the chemical modifications of crosslinked PDMS with hydrophilic polymers. The treatment usually involves introducing functional groups, such as silanol groups and hydridosilane, onto the surfaces, followed by silanization or hydrosilylation of hydrophilic silanes[37] or hydrophilic olefins.[38] In this project, olefin functionalized polyethylene glycol (PEG) was used as the surface passivating polymer to ameliorate the hydrophobicity of PDMS surfaces via hydrosilylation.

### 1.7 Passivation of PDMS Surfaces via PEGylation

*Nonfouling characteristics of PEG.* Polyethylene glycol (PEG) is a water-soluble, non-toxic, and non-immunogenic polymer that is highly mobile in aqueous solutions.[39] Surface PEGylation refers to the process of covalently attaching PEG onto material surfaces, which is a frequently employed strategy to improve material biocompatibility by "masking" material surfaces from direct contact with external biology. Two key benefits of surface PEGylation have been

widely approved by the biomaterials community. First, PEG-modified surfaces resist protein adsorptions;[40-43] second, when forced into direct contacts, proteins are not readily denatured by PEG.[44, 45]

The molecular basis of the nonfouling characteristics of PEG has been investigated in two major perspectives. The "physical" view focuses on the entropic repulsion between surface-tethered PEG and approaching proteins, where steric repulsion due to the compression of the overlayer plays a critical role.[46-49] The "chemical" view, on the other hand, explores the osmotic repulsion exerted by hydration shells formed on the PEGylated surfaces, which energetically suppresses protein adsorptions onto the PEG layer.[50, 51] The two perspectives are by no means mutually exclusive, and together, they suggest that grafting densities, overlayer thickness,[52] chain length, and morphologies[53] of surface-bound PEG molecules are affecting the nonfouling performance of PEGylated surfaces, which become important guidelines of this study.

*PEGylation strategies on PDMS surfaces.* Preparing PEGylated PDMS surfaces first requires functionalization of the inert polymer surface (e.g. with -SiOH or -SiH). This activation step is sometimes complicated by the challenge to preserve the introduced functional groups: -SiOH-embedded PDMS surfaces are prone to hydrophobic recovery, whereas -SiH groups are susceptible to oxidative consumption by the ambient oxidants. Also, in order to introduce proper functional groups to react with functionalized PEG molecules, reaction schemes sometime involve laborious layer-by-layer surface functionalizations,

which compromises the efficiency and reproducibility of surface coverage of PEG[54-57]. Therefore, effective PEGylation designs usually involve reduced steps of surface modifications and proper strategies to preserve incorporated functionalities.

Chen *et al.* reported an effective PEGylation design using classic room temperature vulcanization chemistry.[58] Specifically, monomethyl-ended PEG was conjugated with triethoxysilylpropyl groups (TES), which act as crosslink sites in the synthesis of PDMS networks. In this manner, PDMS thin films are functionalized with PEG during the crosslinking process. In a recent 2010 publication, Mikhail *et al.* proposed another effective scheme[59], where -SiH groups were introduced during the synthesis of PDMS elastomers as the functional moieties of the crosslinkers. The crosslinking reaction was then followed by surface hydrosilylation between functional PEG (allyl-PEG) and residual -SiH. Both designs are favored in part because they eliminate the need to activate the inert PDMS surfaces, which inspired the PEGylation design in this project.

### 1.8 Surface Characterization: Contact Angle and Hysteresis

The degree of surface hydrophobicity/hydrophilicity can be generalized as wettability, that is, the ability of a surface to maintain its contact with a liquid. The concept of contact angle quantifies this otherwise qualitative property, and is used to assess effectiveness of surface PEGylation in this project.

*Theory.* As a liquid droplet is casted onto a solid surface, it takes on the shape that equilibrates the surface tensions of the liquid-solid, liquid-vapor, and solid-vapor interfaces (Figure 5). The equilibrium state can be described by Young's equation:

$$\mathbf{0} = \boldsymbol{\gamma}_{\mathbf{SV}} - \boldsymbol{\gamma}_{\mathbf{SL}} - \boldsymbol{\gamma}_{\mathbf{LV}} \mathbf{cos}\boldsymbol{\theta}_{\mathbf{C}} \quad (1)$$

where $\boldsymbol{\gamma}_{\mathbf{SV}}$, $\boldsymbol{\gamma}_{\mathbf{SL}}$, and $\boldsymbol{\gamma}_{\mathbf{LV}}$ denote the surface tensions of the solid-vapor, solid-liquid, and liquid-vapor interfaces, and $\boldsymbol{\theta}_{\mathbf{C}}$ is the equilibrium contact angle formed by the free interfaces.

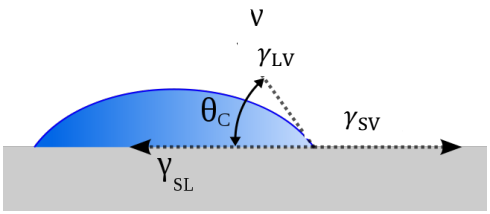


**Figure 5.** Illustration of equilibrium contact angle $\theta_c$.

In theory, a given system of solid, liquid, and vapor at a given temperature and pressure has a unique equilibrium contact angle $\theta_c$. Yet the theoretical condition is based on a few assumptions. First, the solid surface is physically smooth and chemically homogeneous. Second, the liquid drop is neither penetrating the solid surface nor reacting with the surface functional groups. These assumptions are rarely met in reality. As a result, dynamic contact angles are measured to overcome the limitations. As a liquid drop is added to a solid surface, the contact angle that permits maximum liquid volume without increasing the liquid-solid interfacial area is defined as the advancing contact angle $\boldsymbol{\theta}_{\mathbf{A}}$; as the drop is withdrawn form the surface, the angle that allows for the minimum

liquid volume without decreasing the liquid-solid interfacial area is the receding contact angle $\boldsymbol{\theta_R}$. Equilibrium contact angle ($\boldsymbol{\theta_C}$) can be any value between the advancing and receding contact angles, where $\boldsymbol{\theta_A} > \boldsymbol{\theta_C} > \boldsymbol{\theta_R}$.

Generally, on a chemically heterogeneous surface, advancing angle is associated with the low-energy regions (hydrophobic) where the advancing edge of the liquid drop is hindered, and the receding angle is associated with the high-energy regions (hydrophilic) where the receding liquid edge is pinned down. The difference between hydrophobic and hydrophilic regions is known as the contact angle hysteresis.

Contact angle hysteresis results from the deviation of a system from the ideal conditions mentioned earlier. For the PDMS system, the deviation majorly comes from physical roughness and chemical heterogeneity of the surfaces.

Wenzel's equation describes the impact of surface roughness on observed contact angles:

$$\cos \boldsymbol{\theta_m} = \boldsymbol{r} \cos \boldsymbol{\theta} \tag{2}$$

where $\boldsymbol{\theta_m}$ is the observed contact angle, and $\boldsymbol{\theta}$ is the intrinsic contact angle of an ideally smooth surface, and r, the Wenzel's roughness ratio, is defined as the ratio of the actual surface area to the projected area (the area of a smooth surface having the same geometric shape and dimensions[60]. ). Since r is larger or equal to 1, the equation suggests that roughening an intrinsically hydrophilic surface ($\boldsymbol{\theta}$ < 90°) leads to an lower observed contact angle $\boldsymbol{\theta_m}$ compared to the intrinsic

contact angle $\boldsymbol{\theta}$; in the case of a intrinsically hydrophobic surface ($\boldsymbol{\theta} > 90°$), the opposite is observed.

On the other hand, the effect of chemical heterogeneity is described by Cassie's equation:

$$\boldsymbol{\cos \theta_m = Q_1 \cos \theta_1 + Q_2 \cos \theta_2} \quad (3)$$

where $\boldsymbol{Q_1}$and $\boldsymbol{Q_2}$ are fractions of surface with intrinsic contact angles of $\boldsymbol{\theta_1}$ and $\boldsymbol{\theta_2}$. The equation indicates that for a chemically heterogeneous surface, the observed contact angle is a weighted average of the intrinsic contact angles of chemically distinct regions.

Contact angle measurement reveals important information regarding physical and chemical characteristics of a surface before and after surface modifications. It is therefore used to characterize PEGylated PDMS surfaces and PEGylation efficiency in this project.

# 2. EXPERIMENTAL

## 2.1 Materials and Apparati

*General.* Table 1 summarizes the important structural parameters of reagents used for the synthesis and subsequent PEGylation of crosslinked PDMS substrates. Vinyl-terminated polydimethylsiloxanes (V-PDMS), including V41 (V-PDMS-41), V31 (V-PDMS-31), V25 (V-PDMS-25), and V21 (V-PDMS-21), and methylhydrosiloxane-dimethylsiloxane copolymers (PHMS), including PHMS-991, PHMS-301, PHMS-071, PHMS-031 were purchased from Gelest, Inc. (USA) and stored at room temperature. Karstedt's catalyst, platinum-divinyltetramethyldisiloxane complex, was also purchased from Gelest, Inc., diluted in anhydrous toluene to $5\times10^{-4}$ g/mL, aliquoted in 10 mL, and stored in vials wrapped with aluminum foil at -20 °C. Mono-vinyl-terminated polyethylene glycol (V-PEG), including V-PEG$_1$ (degree of polymerization n=1), V-PEG$_2$ (n=2), and V-PEG$_{10}$ (n=10) were purchased from Sigma-Aldrich, Co. (USA).

**Table 1.** Important structural parameters of reagents used for the synthesis and subsequent PEGylation of crosslinked PDMS substrates. "$M_n$" and "$M_v$" specify the number-average molecular weight and the viscosity molecular weight, respectively. "Mole % of -SiH" reports the density of repeat units containing -SiH functionality in PHMS.

| V-PDMS | $M_n$ | PHMS | Mole % of -SiH | V-PEG | $M_v$ |
|---|---|---|---|---|---|
| V-41 | 31350 | 991 | 100 % | V-PEG$_{10}$ | 525 |
| V-31 | 14000 | 301 | 34 % | V-PEG$_2$ | 102.1 |
| V-25 | 8600 | 071 | 6.4 % | V-PEG$_1$ | 88.1 |
| V-21 | 4700 | 031 | 4.0 % | | |

Silicon wafers (100 orientation, P/B doped, resistivity 1–10 Ω-cm, thickness 475–575 μm) were purchased from International Wafer Service, Inc. (USA).

*Instrumentations.* Silicon wafers were oxidized in Harrick plasma cleaner PDC-001 (Harrick Scientific Products, Inc., USA) prior to usage. Spin casting was done using Laurell WS-400B-6NPP/LITE single wafer spin processor (Laurell Technologies Corp., USA) at 6100 rpm for 60 s. Precision 51221126 Gravity Convection Lab Oven (Thermo Fisher Scientific, Inc., USA) and Lab Oven with $N_2$ inlet and vacuum were used for substrate curing without and with $N_2$ purging, respectively. Dynamic contact angles were measured with NRL C.A. 100-00 goniometer (Ramé-hart Instrument Co., USA) with a Gilmont syringe (Gilmont Instrument Co., USA) attached to a 24-gauge flat-tipped needle. Substrate thickness was measured with LSE Stokes Ellipsometer (Gaertner Scientific Corp., USA). Atomic force microscope images were obtained with Veeco Metrology Dimension 3100 Atomic Force Microscope (Veeco Instruments, Inc., USA) under tapping mode with a Veeco silicon tip (resistivity 1–10 Ω-cm, P doped). Surface features analyses were done using the Nanoscope software (Veeco Instruments, Inc., USA).

## 2.2 Methods

### 2.2.1 Preparation of Silicon Wafers

Silicon wafers were cut into 1.3 cm × 1.5 cm, rinsed with distilled water, and dried with compressed air. They were dried further in a clean oven at 110 °C for 30 min, and then treated with oxygen plasma for 15 min.

### 2.2.2 Preparation of Crosslinked PDMS Substrates

Hydrosilylation reactions between vinyl-terminated polydimethylsiloxane (V-PDMS) and methylhydrosiloxane-dimethylsiloxane copolymers (PHMS) were carried out to obtain crosslinked PDMS networks, in the presence of platinum-divinyltetramethyldisiloxane complex (Karstedt's catalyst) (Figure 6). Samples were prepared using V-PDMS of different molecular weights, PHMS compolymer with different percentages of -SiH functionality, and various molar ratios between functional groups on PHMS and V-PDMS ([-SiH]:[Vinyl]).

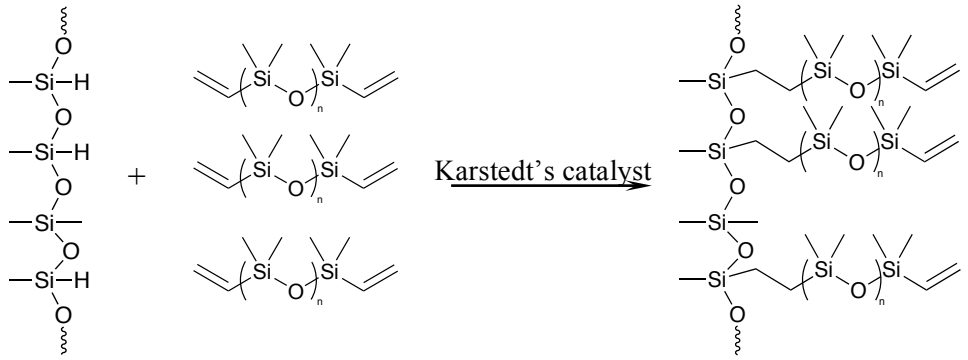


**Figure 6.** Preparation of crosslinked PDMS networks via hydrosilylation between functionalized PDMS pre-polymers PHMS and V-PDMS, in the presence of Karstedt's catalyst.

Crosslinked PDMS substrates were prepared as monoliths for tensile tests and as thin films supported by silicon wafers for characterizations of surface properties. PDMS Monoliths prepared with V-PDMS-31, PHMS-991, and a 1:5 molar ratio of [Vinyl]:[-SiH], for example, were synthesized using the following procedure. 2.800 g of V-PDMS-31 was weighed in a scintillation vial, to which 200 μL of

$5\times10^{-4}$ g/mL Karstedt's catalyst and 0.067 g of PHMS-991 were added sequentially. Each addition was followed by vortexing for 20 s to ensure sufficient mixing. The well-mixed sample was thoroughly de-gassed under $N_2$, poured into a polystyrene petridish, and cured at room temperature for 24 h. To prepare PDMS thin films with the same composition, 70 wt% V-PDMS in toluene was used instead of neat V-PDMS. Immediately after mixing all the components, 100 μL aliquots of diluted mixture were spin-casted onto oxygen-plasma cleaned silicon wafers. The PDMS thin films were then cured in covered petridishes at 90 °C for 2 h or at 110 °C for 1 h.

### 2.2.3 PEGylation on Crosslinked PDMS Thin Films

Cured PDMS thin films supported by silicon wafers were transferred to a clean sample holder, placed in a glass reaction tube (inner diameter: 2.5 cm) fitted with an o-ring and a glass cap. Surface PEGylation was performed in the solutions

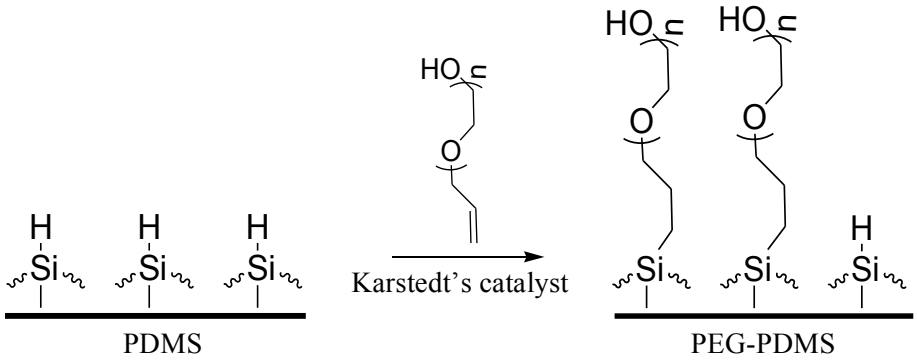


**Figure 7.** Surface PEGylation via hydrosilylation between surface -SiH reactive sites and mono-vinyl-terminated PEG, in the presence of Karstedt's catalyst.

of vinyl-terminated polyethylene glycol (V-PEG) dissolved in acetonitrile, in the presence of a desirable amount of Karstedt's catalyst.

The ratio of V-PEG to acetonitrile was 1:20, 1:10, and 1:2 (by volume) for V-PEG$_1$, V-PEG$_2$, and V-PEG$_{10}$, respectively, to keep a consistent molar concentration of vinyl groups. For all cases, PDMS thin films were treated in the solutions by complete immersion for 24 h. Surface PEGylation occurs via hydrosilylation between surface -SiH groups and vinyl end groups of PEG (Fig. 7). After the reaction, wafers were individually rinsed in toluene, acetonitrile, ethanol, and Milli-Q water sequentially to remove excess reagents from substrate surfaces and dried in vacuum for 12 h.

### 2.2.4 Preparation and PEGylation of PHMS Monolayer

PHMS-991 was drop-casted onto oxygen-plasma treated silicon wafers in aliquots of 100 μL. After 24 h curing at 95 °C, samples were rinsed sequentially with toluene, acetone, and Milli-Q water to remove excess PHMS. Rinsed samples were transferred to a clean sample holder placed in a glass reaction tube (inner diameter: 2.5 cm) and treated with the same PEGylation protocol as on crosslinked PDMS thin films described in section 2.2.3.

## 2.3 Characterizations

### 2.3.1 Mechanical Properties of Crosslinked PDMS Monoliths

*Tensile tests.* Young's moduli of crosslinked PDMS monoliths were determined via tensile tests, where Young's modulus $E$ is defined as the ratio between tensile stress σ and tensile strain ε:

$$E \equiv \frac{\sigma}{\varepsilon} = \frac{F/A}{\Delta l/l_o} \quad (4)$$

$F$ is the applied force, $A$ is the original cross-sectional area of the specimen on which the force is applied, $l_o$ is the original length of the specimen, and $\Delta l$ is the change in length.

24 h after preparation, crosslinked PDMS monoliths were cut into dog-bone shape following the standard dimension of ASTM D638 (measurement region: length 2.00 cm, width 0.80 cm) (Figure 8). Specimen thickness was measured using vernier calipers as an average of three measurements. All specimens were clamped in custom grips, which are designed to allow for maximum contact surface area with the specimen, and to reduce the stress concentration on the specimen near the edges of the grip.

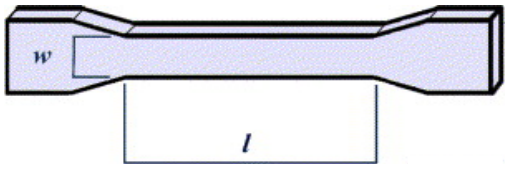


**Figure 8.** Dog-bone shaped crosslinked PDMS monoliths used in tensile tests, based on ASTM D638 standardized dimension.

Incremental weights (10-150 g) were applied to the specimen along the longitudinal axis, and corresponding elongations of the specimen were captured as digital images and analyzed via *ImageJ*. In the resulting tensile stress-strain plot, Young's modulus was the slope of the linear region, where the strain was between 5% and 30%.

### 2.3.2 Surface Characterizations of Crosslinked PDMS Thin Films

*Contact angles.* Dynamic advancing ($\theta_A$) and receding ($\theta_R$) contact angles were measured while Milli-Q water was added to and withdrawn from the pre-casted droplet on the substrate surface, respectively. Each result was reported as an average of at least five measurements with standard deviation.

*Ellipsometry.* Before and immediately after each surface treatment, substrate thickness was measured using ellipsometry. The result for each sample was reported as an average of five different measurements. Specifically, the thickness of a layer of interest (i.e. PHMS or PEG layer) was determined as the difference in substrate thickness after and before treatment.

*Atomic Force Microscopy (AFM).* Surface topography of PEGylated PHMS thin films was characterized via AFM. Images were obtained with a Veeco Metrology Dimension 3100 Atomic Force Microscope under tapping mode, and -analyzed using the *Nanoscope* software.

# 3. RESULTS AND DISCUSSION

## 3.1 Mechanical Tunability of Crosslinked PDMS Monoliths

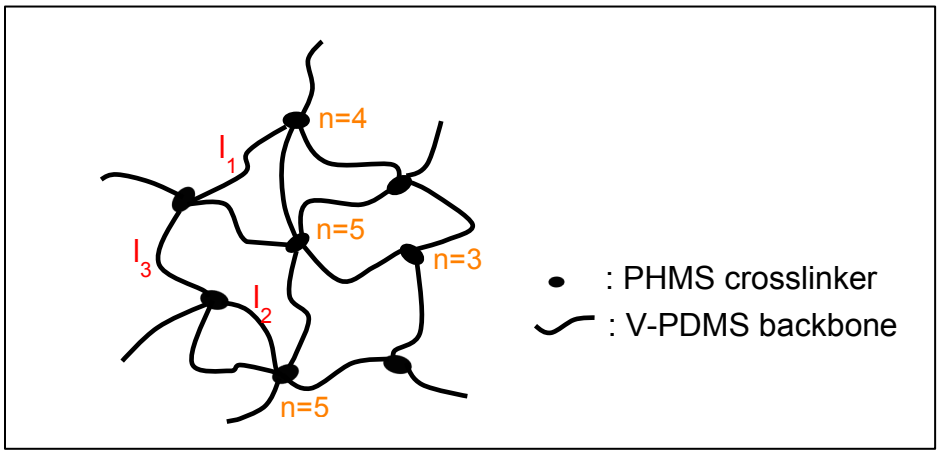


**Figure 9.** Illustration of crosslinked PDMS network consisting of crosslinker (PHMS) and backbone (V-PDMS) pre-polymers.

*Overview.* Our control over the modulus of crosslinked PDMS was guided by the structure-property correlation of a crosslinked network. As illustrated in Figure 9, the mechanical strength of a crosslinked network is impacted by two major parameters: <*l*> the average length of backbones between adjacent crosslinkers, and <*n*> the average number of backbones attached to each crosslinker, or crosslinking density. In this project, vinyl-terminated PDMS (V-PDMS) and methylhydrosiloxane-dimethylsiloxane copolymers (PHMS) are designed to be the backbone and the crosslinker of the network, respectively. Therefore, <*l*> is determined by the molecular weight of V-PDMS, and <n> is dictated by both the density of -SiH moieties on PHMS and the molar ratio between crosslinker and backbone functional groups, (i.e. [-SiH]:[Vinyl]). The

impact of each factor on the modulus of crosslinked PDMS will be elaborated in the following sections.

In this project, all crosslinked PDMS monoliths were prepared using optimized concentration of Karstedt's catalyst (1~7 ppm by weight) to ensure a proper rate of gelation that is high enough but does not interfere with thorough mixing of the pre-polymers.

*Tensile test.* A sample tensile stress versus tensile strain curve is shown in Figure 10. A "Reverse" plot was taken to ensure that substrate elongation due to applied stress was fully elastic and did not cause permanent deformation. Young's modulus was taken as the slope of the linear region with strain between 5-30 %.[61]

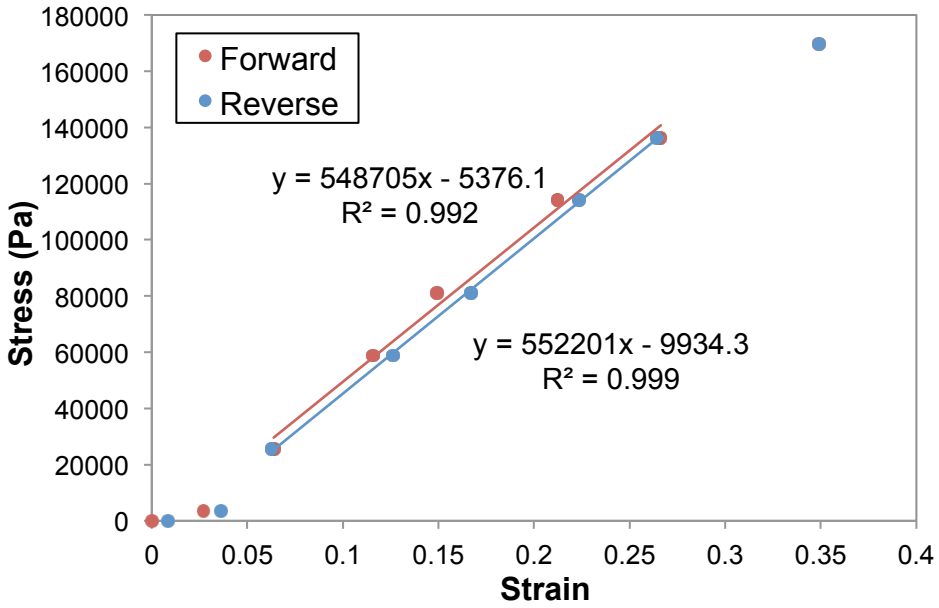


**Figure 10.** A sample tensile stress verses tensile strain curve. "Forward" was taken as incremental weights (0-150g) were applied to the substrate, and "Reverse" was taken as the applied weights were detached sequentially. Young's modulus was reported as the slope of the linear region where strain is between 5-30%.

The high linearity of the plot and the low hysteresis between "Forward" and "Reverse" curves indicate that the stress-strain curve is in the elastic region and has not yet reached the proportionality limit (Figure 4). Therefore, the selected region reflects the elastic property of crosslinked PDMS and can be used to calculate Young's modulus of the substrate.

*Impact of different -SiH density on PHMS crosslinkers.* With the molar ratio between the crosslinker and the backbone functional groups ([-SiH]:[Vinyl]) kept as 5:1, crosslinked PDMS monoliths were prepared using four different types of PHMS crosslinkers. As shown in Figure 11 and Table 2, given the same number of total repeating units (i.e. 24), the crosslinkers differ in the density of the repeat units containing -SiH moieties (or -SiH density). As the density decreased, Young's moduli of crosslinked PDMS monoliths decreased until no gelation occurred (Table 2). The trend reflects the drop in the average number of backbones attached per each crosslinker (<n>), which can be estimated based on the number of -SiH groups per PHMS molecule ($x$) and the [-SiH]:[Vinyl] ratio. For PHMS-991, for example, a total number of 24 -SiH groups per molecule and a 5:1 molar ratio of [-SiH]:[Vinyl] give rise to approximately 24/5≅5 V-PDMS backbones per crosslinker, leading to the substrate modulus of 534 kPa. For PHMS-301, PHMS-071, and PHMS-031, <n> decreases to 2, 0.4, and 0.2 respectively.

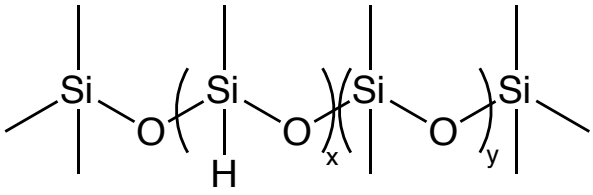


**Figure 11.** Chemical structure of the PHMS crosslinker, a statistical copolymer of methylhydrosiloxane and dimethylsiloxane. For all crosslinkers, $x$+$y$=24.

**Table 2.** Young's modulus of crosslinked PDMS as a function of -SiH density on PHMS. For all samples, V-PDMS-31 (28 kDa) was used as the backbone pre-polymer and [-SiH]:[Vinyl] was kept as 5:1. (* indicates the highest modulus observed for substrates prepared with PHMS-071 and V-PDMS-31.)

| Crosslinker Identity | -SiH Density | | Modulus (kPa) |
|---|---|---|---|
| | $x/(x+y)$ | $x/Molecule$ | |
| PHMS-991 | 100% | 24 | 534 |
| PHMS-301 | 34% | 8 | 356 |
| PHMS-071 | 6.4% | 2 | 69* |
| PHMS-031 | 4% | 1 | No gelation |

In addition, for PDMS monoliths prepared with PHMS-991 and PHMS-301, gelation occurred consistently within 20 min after preparation, whereas significant variation in gelation rate was observed for monoliths prepared with PHMS-071, leading to final products with low or no gelation.

The observed discrepancies among different types of PHMS crosslinkers can be explained by the difference in the maximum number of backbones that can possibly attach to a crosslinker ($x$). In theory, ineffective crosslinking occurs as the number of backbones attached to a crosslinker is below 3. For PHMS-071, the highest possible number of backbones that can attach to a PHMS-071 molecule is 2 (Table 2), leading to ineffective crosslinking and the observed inconsistency in substrate moduli. For PHMS-991 and 301, on the other hand, $x$ values are far

above 3 so that effective crosslinking dominates. Therefore, considering the consistency of the moduli of crosslinked PDMS products, PHMS-991 and PHMS-301 were selected as effective crosslinkers for further studies.

*Impact of [-SiH]:[Vinyl].* To vary the ratio between crosslinker and backbone functional groups ([-SiH]:[Vinyl]), crosslinking reactions were carried out between various amounts of PHMS-991 or PHMS-301 and a fixed amount of V-PDMS of 28 kDa (V-PDMS-31). Gelation does not occur for mixtures with no excess -SiH groups (i.e. [-SiH]:[Vinyl] ≤ 1), indicating that not all of -SiH groups on the PHMS crosslinkers are accessible for reactions with V-PDMS pre-polymers. Such observation that the number of active functionalities ($x$) is higher than the number of effective ones ($x_e$) is commonly observed for high-functionality crosslinkers[62-65] and is most likely due to steric effects. In addition, excess -SiH groups were reported to be susceptible to oxidation by ambient water and oxygen molecules.[66] however, no detectable change in substrate modulus was observed up to seven days after preparation.

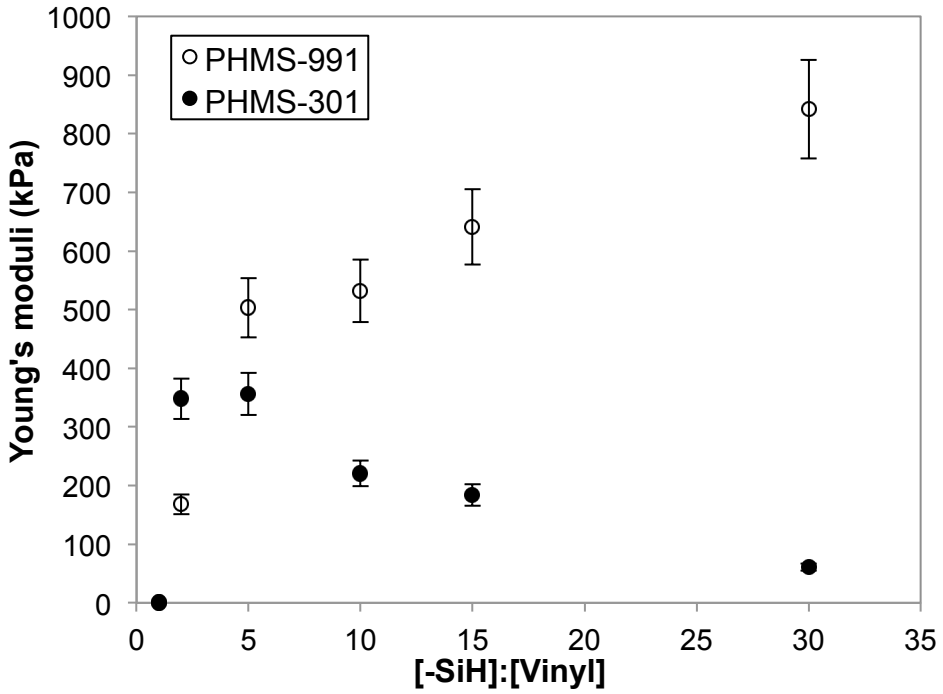


**Figure 12.** Young's moduli of crosslinked PDMS monoliths as a function of the ratio between crosslinker and backbone functional groups ([-SiH]:[Vinyl]).

It is noteworthy that substrates prepared with PHMS-991 and PHMS-301 exhibit different trends as the ratio of the mutually reactive functional groups was varied (Figure 12). For PHMS-991, an increase in [-SiH]:[Vinyl] leads to a monotonic increase in substrate modulus, whereas for the PHMS-301 series, substrate modulus peaks as [-SiH]:[Vinyl] reaches 5 and decreases with further increase in the ratio.

An increase in [-SiH]:[Vinyl], or PHMS concentration, results in a higher crosslinker concentration but a lower average number of V-PDMS backbones attached per PHMS molecule (<n>). The opposing effects of these two structural parameters on substrate moduli lead to a trade-off between the two, where the

dominating parameter dictates the trend of substrate moduli. For PHMS-991, the increasing crosslinker concentration dominated the trend up to the highest [-SiH]:[Vinyl] ratio examined. For the PHMS-301 series, on the other hand, the maximum modulus was observed as the decreasing average number of backbone molecules per crosslinker took control over the increasing concentration of crosslinkers. Since -SiH density is the only difference between PHMS-991 and PHMS-301, it is most likely the contributing factor to the distinction between the two trends. Specifically, there are ~8 -SiH in each PHMS-301 molecule compared to ~24 in each PHMS-991, leading to a low average number of backbones attached per PHMS-301 (<n>) to start with (i.e. as [-SiH]:[Vinyl] = 1). As a result, as [-SiH]:[Vinyl] increases, the effectiveness of PHMS-301 molecules as crosslinkers soon drops with the decreasing <n>, which was not observed in the PHMS-991 series. It should be noted, however, that crosslinker effectiveness cannot be solely accounted for by <n>, since PHMS-991 molecules apparently remain as effective crosslinkers even as [-SiH]:[Vinyl] reaches 60 (corresponding to <n> = 0.4). The robustness of PHMS-991 as an effective crosslinker can be attributed to its wide range of possible n values (0~24), such that even with a relatively low number of backbones attached per crosslinker *on average*, any crosslinked locality across the substrate with a n value higher than 3 will contribute to the overall stiffness of the substrate.

In brief, [-SiH]:[Vinyl] proves to be an effective parameter to readily manipulate the moduli of crosslinked PDMS monoliths. The robustness of

PHMS-991 molecules as effective crosslinkers can be taken advantage of to produce high-modulus substrates (up to ~1000 kPa), whereas PHMS-301 can be used to fine-tune modulus at the lower end of the spectrum (< 400 kPa).

*Impact of molecular weight between crosslinkers.* Model networks formed by the crosslinking reaction between functionally-terminated polymers of known molecular weight and crosslinker molecules of known functionality were first exploited by Mark *et al.* in 1977.[67] The model has since been employed for preparing crosslinked polydimethysiloxane,[68] polyurethaneor,[69,70] and polyisobutylene[71] networks, where the molecular weight between adjacent crosslinkers ($M_c$) was reported to be identical to the number-average molecular weight ($M_n$) of the functionally-terminated polymer. The design therefore provides a powerful tool to obtain quantitative information ($M_c$) regarding structural properties of a crosslinked network, which would otherwise be a challenge to estimate in randomly crosslinked networks.[72]

Our design of crosslinked PDMS networks follows the model system described above. Therefore, the number-average molecular weight of V-PDMS should provide a reasonable estimate of the molecular weight between adjacent crosslinkers. It is not surprising that the modulus of crosslinked PDMS is inversely proportional to the molecular weight of V-PDMS for substrates prepared with both types of crosslinkers (Figure 13). It should be noted, however, that the molecular weight dependence is not as significant for substrates prepared using PHMS-301 as for those prepared using PHMS-991, most likely due to the

lower average number of backbones attached per PHMS-301, as the molar ratio between -SiH and vinyl ends is maintained at 5.

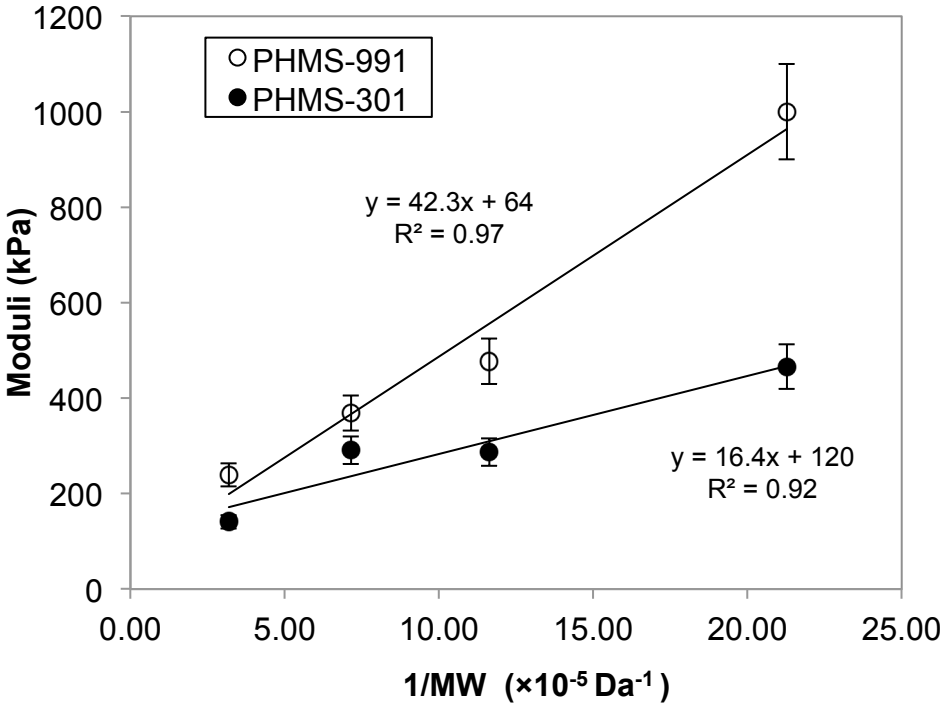


**Figure 13.** Young's Moduli of crosslinked PDMS monoliths as a function of the number-average molecular weight of V-PDMS. For all samples, [-SiH]:[Vinyl] = 5.

In a 2004 review, Larsen *et al.* compared results obtained from 58 different articles studying elastic moduli of crosslinked PDMS prepared by crosslinking functionally-terminated PDMS pre-polymers.[73] All collected data was fitted into the Langley-Graessley (L-G) model:[74, 75]

$$\mathrm{E} = \left(1 - \frac{2}{f}\right)\frac{\rho \mathrm{RT}}{\mathrm{M_c}} + \mathrm{G_o T}_E \qquad (5)$$

where E is the elastic modulus of a crosslinked network, $M_c$ is the average molecular weight between crosslinks, $f$ is the average number of backbones

attached per crosslinker, ρ is the density of PDMS, R is the ideal gas constant, T is the absolute temperature, $G_o$ is the plateau modulus of the uncrosslinked, high molecular weight pre-polymer, and $T_E$ is the proportion of the maximum concentration of topological interactions contributing to the elastic modulus. Essentially, the L-G model stemmed from the phantom model:

$$\mathrm{E} = \left(1 - \frac{2}{f}\right)\frac{\rho \mathrm{RT}}{\mathrm{M_c}} \tag{6}$$

where the contribution of physical entanglements of polymer chains to the overall elastic modulus was neglected. However, experimental results have shown that the impact of such physical entanglements becomes pronounced as molecular weight of PDMS pre-polymers increases, leading to the commonly observed deviation of experimental data from predictions made by the phantom model. Therefore, by introducing the additional $G_oT$ term, Langley and Graessley took into account both chemical crosslinks and physical entanglements of polymer chains as contributing factors to the overall modulus of a crosslinked network.

Given the L-G model, Larsen *et al.* fitted the literature results into the following equation:

$$\mathrm{E} = \left(1 - \frac{2}{f}\right)\frac{a}{\mathrm{M_c}} + b \tag{7}$$

where a, b were extracted as empirical parameters from the least square fits. Theoretically, *a* reveals the contribution of the crosslink junctions to the overall elastic modulus, which should be close to ρRT (Eq. (5)), while *b* represents the impact of physical entanglement of polymer chains. Therefore, using data

obtained with $M_c$ ranging from 660 to 84, 000 Da, Larson *et al* reported *a* and *b* to be $(23.6 \pm 0.6) \times 10^5$ kPa•Da and 142 ± 7 kPa, respectively.

Therefore, using equation (7), we attempted to extract values of *a* and *b* for the PHMS-301 and the PHMS-991 series, respectively, from the established relationship between substrate moduli and the average molecular weight between adjacent crosslinkers (Fig. 12). Specifically, in order to obtain *a*, theoretical values of *f* were used as the ratio between the total number of -SiH groups per crosslinker and the [-SiH]:[Vinyl] ratio. In other words, $f$ was considered as equivalent to <n> used in the earlier discussions (i.e. the average number of backbones attached per crosslinker). As shown in Table 3, there is good agreement between the *b* value extracted from the PHMS-301 series and the reported value. The *a* value, however, cannot be determined since the model assumes that effective crosslinking only occurs as the average number of backbones attached per crosslinker is higher than 3, and therefore only applies to systems with $f \geq 3$. The dilemma revealed that the actual *f* value that effectively contributed to the elastic modulus for the PHMS-301 series may be higher than the theoretical average number of backbones attached per crosslinker. Therefore, considering that *a* (i.e. ρRT) is relatively consistent among PDMS networks independent of different numbers of *f*-functionalities of crosslinkers and varying molecular weights between adjacent crosslinkers, we calculated the experimental value of *f* for the PHMS-301 series, using the reported *a* value. As a result, *f* was determined to be 6.5 for PDMS networks prepared with PHMS-301 and a 5:1

ratio between [-SiH] and [Vinyl]. This value gives us a better estimate of the average number of backbone polymers attached per PHMS crosslink that is effectively contributing to the elastic modulus of the crosslinked network. It is interesting to realize that this value is considerably higher than our expected value of average number of backbones attached per PHMS-301 crosslinker (<n> = 2). The deviation confirms our earlier speculation, that is, even though <n> is an informative parameter to predict the mechanical property of crosslinked PDMS, substrate modulus does not depend on <n> alone. Rather, the mechanical property is determined by the effective crosslinks that dominate the network. In the case of PHMS-301, such dominating crosslinks have ~6 backbone polymers attached on average.

On the other hand, relatively large discrepancy was observed between *b* extracted from the PHMS-991 series and the reported value. Such discrepancies can be explained from two major aspects. First, since *b* reveals the impact of physical entanglement of polymer chains on the overall elastic modulus, a dependency of *b* on *f* is expected as mentioned by Larson *et al*. While the *b* value reported in the review presents an average of data obtained using numerous types PHMS crosslinkers with *f* ranging from 3 to over 40, the correlation between *b* and *f* was not studied and might explain the observed discrepancy in our study. Second, the PHMS-991 series in our study deviates, to certain extend, from the assumptions made by the model. As commented by Larson *et al.*, the model was built only for "the strongest network obtainable" given specified types of

crosslinker and backbone pre-polymers. Simply put, the model was restricted to networks that were prepared with a stoichiometry between crosslinker and backbone functional groups that gave rise to the maximum substrate modulus. In our case, with given types of V-PDMS and PHMS pre-polymers, such stoichiometry corresponds to the [-SiH]:[Vinyl] ratio that leads to highest Young's modulus of the substrate. For the PHMS-301 series, the required [-SiH]:[Vinyl] ratio is ~5 (Fig.12), which coincides what we used for the fit. For PHMS-991, on the other hand, the modulus of substrates prepared as [-SiH]:[Vinyl] = 5 is far from the highest possible modulus (Fig.12), which may have contributed to the deviation from the reported values. It is therefore not too surprising that the value of *a* extracted for the -991 series does not agree with the reported value (Table 3).

Therefore, to have a better estimate of the value of *a* and *b* for the PHMS-991 series as for the -301 series, further studies are required to pinpoint the [-SiH]:[Vinyl] ratio that leads to highest possible substrate modulus. Based on current results, this ratio is higher than 60.

**Table 3.** Empirical parameters, *a* and *b*, extracted for the PHMS-301 and the PHMS-991 series, respectively, using the Langley-Graessley model. (* *a* cannot be extracted for PHMS-301 series as *f* is estimated to be 2, since the model only applies to systems with $f \geq 3$.)

| | ***f*** **(Theoretical)** | ***b*** **(kPa)** | ***a*** **(× $10^5$ kPa•Da)** |
|---|---|---|---|
| Reported | 3 ~ >40 | 142 | 23.6 |
| PHMS-301 | 2 | 120 | N/A* |
| PHMS-991 | 5 | 64 | 70.5 |

In summary, Young's modulus of crosslinked PDMS is inversely proportional to the average molecular weight ($M_c$) between adjacent crosslinkers. The proportionality factor correlates the mechanical property with the key structural parameter of PDMS networks, and hence can be used to design formulations of pre-polymer mixtures to fabricate substrates with targeted moduli.

### 3.2 Surface PEGylation on Crosslinked PDMS Thin Films

*Overview.* As mentioned in section 1.6, a recently reported PEGylation scheme by Mikhail *et al.* eliminated the activation step on the inert PDMS surfaces by incorporating -SiH functionalities during the synthesis of PDMS elastomers. Specifically, Sylgard 184 was used to synthesize PDMS networks, where -SiH functionalities were introduced via the addition of methylhydrosiloxane-dimethylsiloxane copolymers (PHMS) to the normal kit recipe. In this project, instead of using the commercial kit, crosslinked PDMS thin films were prepared following the same reaction scheme described in section 3.1. The purpose of this adjustment is two-fold: first, to avoid complicating PDMS surface chemistry with the additives present in the kit, and second, to take advantage of the mechanical tunability of crosslinked PDMS rendered by the design as discussed in section 3.1. Moreover, -SiH functionalities are automatically introduced during the crosslinking reactions, since proper gelation always requires excess -SiH groups relative to vinyl functionalities. Therefore, -SiH surface densities can be readily controlled with [-SiH]:[Vinyl] ratios used in the synthesis of crosslinked PDMS thin films. Surface PEGylation was then

carried out using the pre-incorporated -SiH groups on PDMS surfaces and mono-vinyl-terminated PEG (V-PEG) via platinum-catalyzed hydrosilylations. PEGylation efficiency was studied as a function of the surface density of -SiH, the molecular weight of functionalized PEG, and the concentration of Karstedt's catalyst. The impact of each factor will be elaborated in the following sections.

*From Monoliths to Thin Films of Crosslinked PDMS*. A *thin film* refers to a material thickness from fractions of a nanometer to several micrometers.[76] Since the length scale in one dimension is much smaller than in the other ones, thin film properties, including mechanical elasticity, can be very different from bulk properties of the same material.[77, 78] Using AFM nano-indentation and a modified JKR model,[79] Xu *et al.* observed an exponential increase in Young's modulus with decreasing sample thickness for crosslinked PDMS thin films below 1 μm in thickness; however, thin film moduli started to approach those of the bulk substrates as thin film thickness reached 900 nm.[80] In addition, previous studies of cells on compliant hydrogels have demonstrates that cells may be capable of "sensing" an underlying rigid substrate such as silicon wafers. For mesenchymal stem cells, which can exert matrix stress of hundreds of mironewtons per square micrometer, which is higher than most other cell types, the estimated depth to which cells can sense is 1-3.4 μm.[81, 82] Therefore, thin films need to have at least micron-scale thickness to preserve the mechanical properties of their bulk counterparts, and to avoid the interference of the supporting material.

In this project, a fellow group member Mimi Hang studied the thickness of crosslinked PDMS thin films prepared by spin cast as a function of the pre-polymer weight percentage in toluene. Based on her results, 70% was selected for this project because it gave rise to thin film thickness of ~ 6 μm with relatively smooth surface topography. In this manner, we aim to translate crosslinked PDMS monoliths to their thin film counterparts with preserved mechanical properties.

*-SiH Density.* The impact of -SiH surface density on PEGylation efficiency was first tested with mono-vinyl-functionalized PEG monomers (V-$PEG_1$). Supported PDMS thin films with low and high -SiH surface densities were prepared using 1:5 and 1:10 molar ratios between [Vinyl] and [-SiH] in the pre-polymer mixtures, respectively. In addition, since -SiH groups are susceptible to oxidative consumptions with prolonged exposure to ambient oxidants, different thin film curing temperatures were compared for better preservation of the surface -SiH functionality. Advancing ($\theta_A$) and receding ($\theta_R$) contact angles were measured on PDMS surfaces before and after PEGylation, As expected, unmodified PDMS showed characteristically high advancing and receding contact angles with low hysteresis ($\theta_A/\theta_R = 109°\pm2°/95°\pm1°$). As shown in Figure 14 (a), an increase in surface -SiH leads to a greater drop in surface receding contact angles after PEGylation. With the same -SiH density, PEGylation on PDMS thin films cured at a lower temperature (90 °C) further reduced the receding contact

angles. The decrease in receding contact angles suggests the improved hydrophilic characters of the PEGylated surfaces as discussed in section 1.8.

While a higher -SiH density apparently provides more reactive sites for V-$PEG_1$ molecules, a lower PDMS curing temperature help preserve the reactive -SiH sites from oxidation. Specifically, the two compared curing temperatures (90/110 °C) are kept lower and higher than the boiling point of water, respectively. The oxidative consumption of -SiH was reported to take place in the following sequence:

$$\text{-SiH} \xrightarrow{\text{Oxidation}} \text{-SiOH} \xrightarrow{\text{Condensation}} \text{-SiOSi}$$ [59]

Therefore, a temperature that is higher than the boiling point of water would promote the self-condensation of -SiOH, driving the reaction to the right. The curing condition at 90 °C was thus adopted for further studies.

For PEGylation with mono-vinyl-functionalized PEG dimers (V-$PEG_2$), similar dependence on -SiH density and PDMS curing temperatures were observed (Figure 14 (b)), but the difference between the examined conditions is not as pronounced as in the case of V-$PEG_1$. However, under all examined conditions, no significant decrease in advancing contact angles was observed (Figure 14 (c) (d)), indicating that a considerable fraction of post-PEGylated surfaces is still occupied by the hydrophobic PDMS segments based on Cassie's equation (Eq. (3)). Meanwhile, further increase in V-PEG concentration did not reduce the advancing contact angles (data not shown).

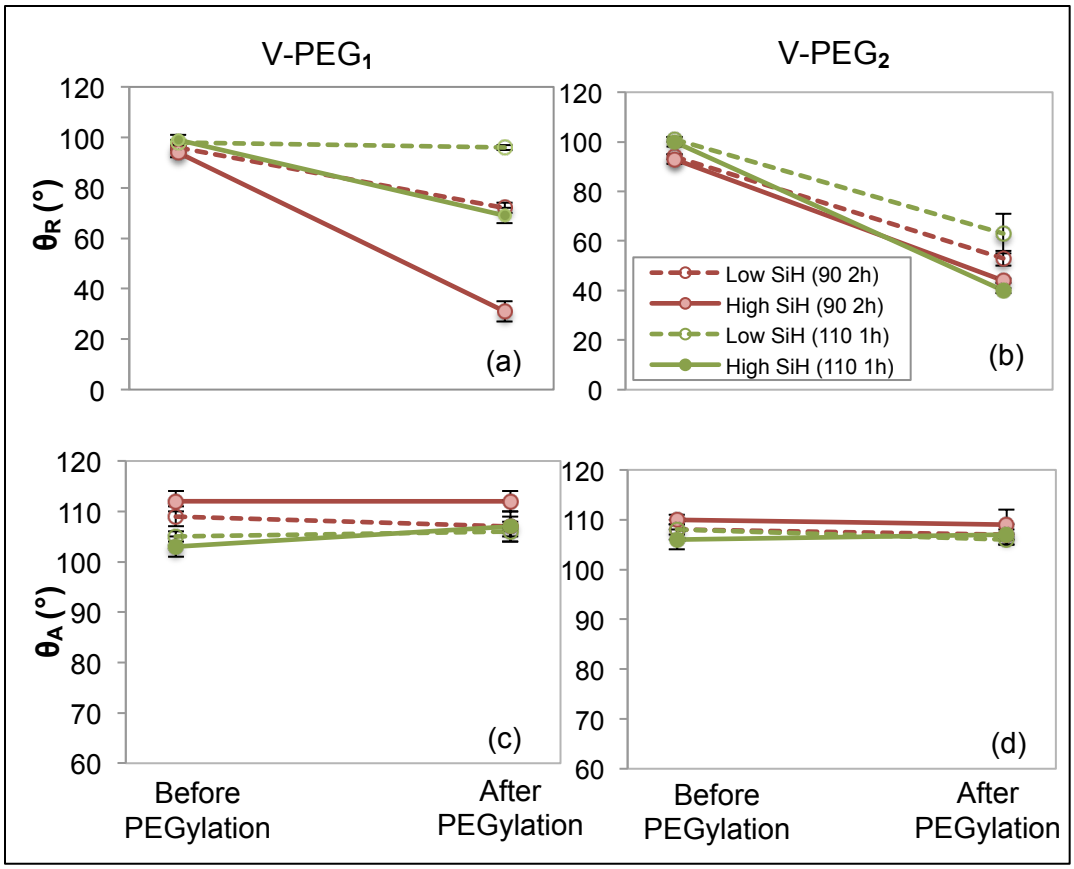


**Figure 14.** Receding (a)(b) and advancing (c)(d) contact angles of crosslinked PDMS thin films with different -SiH surface density before and after PEGylation. Mono-vinyl-functionalized PEG monomers (V-PEG$_1$) and dimers (V-PEG$_2$) were used for surface PEGylation, respectively. Thin films with "High -SiH" density were prepared using 1:10 molar ratio of [Vinyl]:[-SiH], whereas those with "Low -SiH" were prepared using 1:5 molar ratio. PEGylation efficiency was also compared between PDMS thin films cured at 90 °C for 2 h and at 110 °C for 1 h.

The increased hysteresis between advancing and receding contact angles after PEGylation is likely the combined result of the increase in physical roughness and chemical heterogeneity of PEGylated PDMS. As suggested by Chen *et al.*, a rougher surface results from the built-up in the interfacial strain as incompatible materials are forced together.[58] In our case, hydrophobic PDMS surfaces approached by water-soluble PEG would introduce such interfacial

strain. The chemical heterogeneity suggested by the high contact angle hysteresis, on the other hand, implies insufficient surface coverage of grafted PEG. In this project, while the increase in surface roughness is inevitable, chemical heterogeneity can be ameliorated by improving surface coverage of PEG.

Multiple factors can lead to inadequate PEG coverage. Non-ideal conditions for surface hydrosilylation, including low -SiH densities and catalytic activities, could lead to inefficient PEGylation. Moreover, even with a moderate coverage of grafted PEG, the molecular weight of PEG and, more importantly, its corresponding morphology[53] would also come into play in determining the wettability of PEGylated-surfaces. The impact of these factors will be discussed in the following sections.

*-SiH Preservation and Oxygen co-catalysis.* PDMS thin films were cured at 90 °C for 2 h for better preservation of surface -SiH groups. This curing condition was checked to ensure proper gelation of the thin films. In addition, $N_2$ purging was experimented as an additional strategy to preserve surface -SiH groups by lowering ambient $O_2$ level.

As shown in Table 4, PDMS thin films gelled after being cured at 90 °C for 2 h. The modulus (568 kPa) of their monolithic counterpart cured under the same conditions is close to the moduli of PDMS monoliths prepared under the standard conditions (24 h curing at room temperature without $N_2$ purge, $V_{cat.}$ = 200 μL), indicating complete gelation.

It is noteworthy, however, that $N_2$ purge significantly slows down the gelation rate for both thin films and monoliths of crosslinked PDMS (Table 4), which reveals the essential role of $O_2$ in the Pt-catalyzed hydrosilylation. As proposed by Lewis, oxygen coordinates with platinum-based catalyst during the induction period of hydrosilylation and acts as a co-catalyst for the reaction. Therefore, even though $O_2$ deprivation due to $N_2$ purge might have helped preserve surface -SiH groups, it apparently retarded catalytic activities, and is therefore non-ideal.

**Table 4.** Evaluations of curing condition of PDMS thin films for complete gelation and maximum preservation of surface -SiH functionality. For all samples, [SiH]:[Vinyl] = 5, pre-polymers wt % = 70%. [Cat.] = $5\times10^{-5}$ g/mL.

| Cat. Volume (μL) | Curing temp. (°C)/Curing time (h) | $N_2$ purge | Gelation time (h) | Monolith modulus (kPa) |
|---|---|---|---|---|
| 200 | RT/24 | - | N/A | 560 |
| 150 | 90/2 | - | 2 | 568 |
| 150 | 90/2 | + | No gelation | 495 |

*Molecular Weight of V-PEG.* The impact of PEG molecular weight on improving the hydrophilic character of PDMS surfaces was examined using PEG with different degree of polymerization (n=1, 2, and 10, respectively). As shown in Figure 15, V-PEG$_{\mathbf{1}}$**,** with the lowest molecular weight, gave rise to the largest drop in surface receding contact angles after PEGlylation, whereas V-PEG$_{\mathbf{10}}$ led to a comparatively smaller drop. Again, advancing contact angles remained high after PEGylation for all conditions examined.

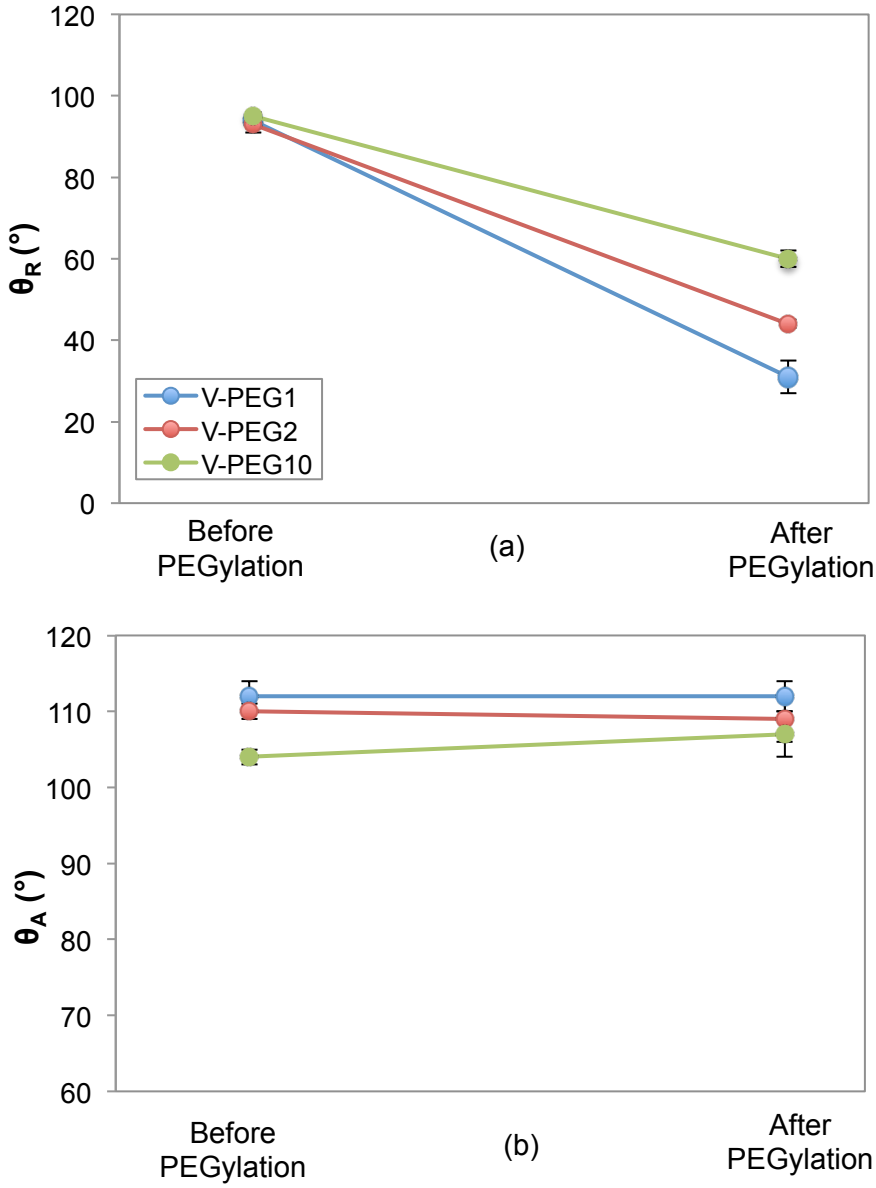


**Figure 15.** Receding (a) and advancing (b) contact angles of PDMS thin films before and after PEGylation with V-PEG$_1$, V-PEG$_2$, and V-PEG$_{10}$, respectively. All PDMS thin films were prepared with a 1:10 molar ratio of [Vinyl]:[-SiH], and cured at 90°C for 2 h.

Although polymer coils with longer chain length will presumably occupy larger surface areas compared to those with lower molecular weights, the overall

coverage of PEG can only be improved if the grafting density is not significantly compromised by the steric effect between high molecular weight molecules.

Moreover, more surface conformations are possible V-$PEG_{10}$ compared to PEG monomer or dimer. The "brush" conformation of shorter chains (i.e. V-$PEG_1$, V-$PEG_2$) makes sure that end hydroxyl groups are exposed to the material surfaces. V-$PEG_{10}$, on the other hand, is more likely to take the "random coil" conformation, which not only poses considerable steric hindrance to the incoming PEG molecules, but also may have buried the hydrophilic hydroxyl group under the hydrophobic ether groups of PEG.[83] In either case, the hydrophilic character of surfaces will not be improved as effectively as with lower molecular PEG.

*Fine-tuning PEGylation on PHMS Monolayers.* As discussed in the previous sections, contact angle measurement reveals important information about both physical and chemical properties of a surface. It, however, faces its limitations. For our purposes, high contact angle hysteresis observed on PEGylated-PDMS likely results from the increase in both the physical roughness and/or the chemical heterogeneity of treated surfaces. The relative contributions from the two factors, however, cannot be differentiated by contact angle measurements alone. Therefore, to have a better insight of the PEGylated surfaces, ellipsometry and Atomic Force Microscopy (AFM) are needed to characterize the grafted thickness and physical topography on PEGylated PDMS, respectively.

However, in our study, the thickness (~6 μm) of crosslinked PDMS thin films approaches the maximum measurable thickness of the ellipsometer

(0~60000 Å). Meanwhile, the characteristic adhesiveness of crosslinked PDMS poses challenges for tapping-mode AFM characterizations. Therefore, instead of using crosslinked PDMS as the substrate material, PHMS monolayers were used to fine-tune surface PEGylations. The adjustment was based on two major considerations. To begin with, PHMS monolayers mimic the chemical characteristics of PDMS thin films: PHMS has the same alternating Si-O backbone as PDMS polymers; -SiH moieties on the methylhydrosiloxane units would be exposed to substrate surfaces, which resembles the surface condition of crosslinked PDMS thin films. Specifically, PHMS-991 with 100% -SiH density was used, theoretically maximizing the surface density of -SiH groups. Secondly, the covalently attached PHMS layer on silicon wafer demonstrates a characteristic thickness of ~35 Å and reduced surface adhesiveness, which allows for proper characterization of ellipsometry and AFM. The major setback of using PHMS as a simplified PDMS analogue is the loss of mechanical control, which will be regained as the optimized PEGylation conditions are translated back to the crosslinked thin films.

*Optimization of Catalyst Concentrations.* To improve PEGylation conditions for better PEG coverage, concentration of Karstedt's catalyst was fine-tuned as a key parameter of surface hydrosilylation. A baseline level of 1.3 ppm (by the weight of Pt catalyst) was used in the earlier part of the thesis studies, whereas an excess level (>300 ppm) was used in some published studies.[58, 59] A gradient of catalyst concentrations was therefore screened for an optimal PEG

coverage. PEGylation efficiencies were evaluated in terms of surface wettability, thickness of PEG layers, and surface topography of PEGylated-PHMS.

As shown in Figure 16, an increasing catalyst concentration used in surface PEGylation led to a monotonic increase in the resulting PEG layer thickness. As for surface wettability, a significant drop in both advancing and receding contact angles occurred as catalyst concentration reached 25 times of the baseline level. With further increase in catalyst concentration, both angles plateaued, and the plateau values ($\theta_A/\theta_R$: 65.5±5°/43.2±3°) are close to literature values. [59]

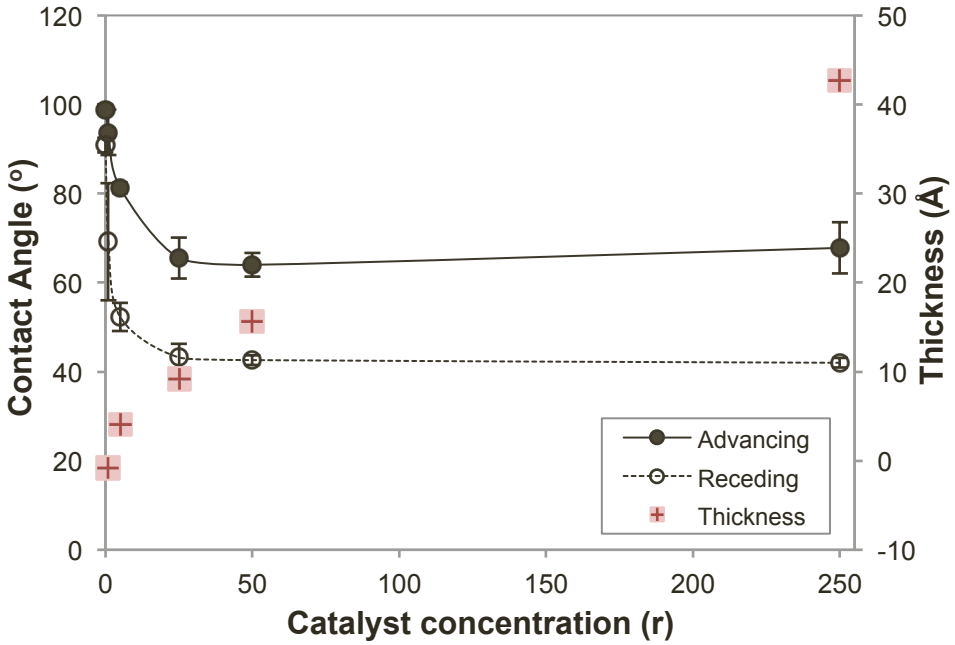


**Figure 16.** Thickness of grafted PEG layers and dynamic contact angles of PEGylated PHMS as a function of Karstedt's catalyst concentrations used in 24-h surface PEGylation. For all samples, mono-vinyl-functionalized PEG decamers (V-PEG$_{10}$) were used for PEGylation. "r" represents the ratio between experimental catalyst concentration and baseline catalyst concentration (1.3 ppm).

Meanwhile, the theoretical monolayer thickness of V-PEG$_{10}$ was calculated using Kuhn's model: [84]

$$r_o = bN^{0.5} = 7.6\ \text{Å} \times (10 \times 3.5\ \text{Å} / 7.6\ \text{Å})^{0.5} = 16.3\ \text{Å} \quad (5)$$

where $r_o$ is the root-mean-square end-to-end distance of a polymer coil, b (7.6 Å) is the reported size of a Kuhn step of PEG molecules, and N is the number of Kuhn steps in a PEG decamer. The catalyst concentration corresponding to 50 times of the baseline level (67 ppm) was therefore pinpointed as an optimal condition, because it gives rise to a monolayer thickness of PEG$_{10}$, and has advancing and receding contact angles residing in the plateau region.

AFM characterizations further confirmed our choice of catalyst concentration. As shown in Figure 17, surface features due to PEGylation only became pronounced as catalyst concentration reached 25 times of the baseline level, accompanied by a noticeable increase in surface roughness. The change in surface topography suggests the change in surface properties, which corresponds to the observed drop in surface contact angles (Figure 16). As catalyst concentration further doubled (50×, 65 ppm), features of grafted PEG became denser and more homogeneously distributed, agreeing with the monolayer thickness reported earlier. Local aggregates of PEG may occur at a higher catalyst concentration, leading to the observed increase in PEG layer thickness.

For the purpose of this project, a monolayer of PEG is desirable. Therefore the corresponding catalyst concentration was selected for further studies.

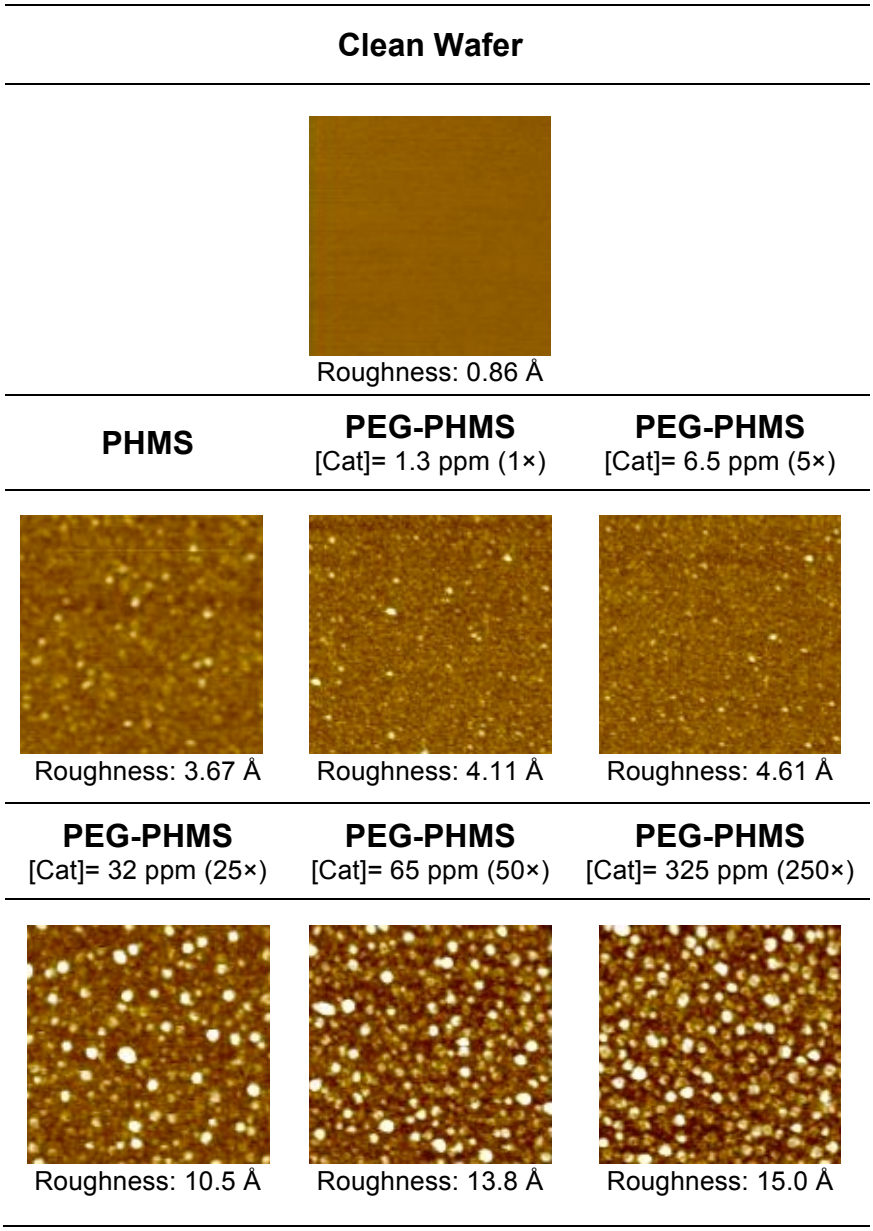


**Figure 17.** AFM images (1.25 μm × 1.25 μm, height scale: 10 nm) of PEGylated PHMS surfaces after 24 h PEGylation at different catalyst concentrations. All samples were treated with V-$PEG_{10}$.

# 3. CONCLUSIONS AND FUTURE DIRECTIONS

This project focused on studying two major aspects of crosslinked polydimethylsiloxane (PDMS) networks: the mechanical tunability and the surface passivation. Crosslinked PDMS was prepared via hydrosilylation between vinyl-terminated PDMS (V-PDMS) and methylhydrosiloxane-dimethylsiloxane copolymers (PHMS) in the presence of Karstedt's catalyst. Monolithic substrates with tunable moduli ranging from 50 to 1000 kPa can be fabricated by manipulating the well-controlled pre-polymer formulations. In addition, -SiH groups can be incorporated into the otherwise inert PDMS networks as residual functionality of hydrosilylation reaction, and were utilized for subsequent surface modifications. Surface PEGylation was thus carried out between surface -SiH and mono-vinyl-terminated polyethylene glycol (V-PEG) on crosslinked PDMS thin films via platinum-catalyzed hydrosilylation. Surface coverage of grafted PEG was improved with proper preservation of surface -SiH groups and optimal concentration of Karstedt's catalyst.

*Mechanical tunability.* In our design, the mechanical tunability of crosslinked PDMS comes from the control over the structural parameters of a crosslinked network. These parameters are directly dictated by the formulation of pre-polymers mixtures in the crosslinking reaction (i.e. hydrosilylation). An inverse proportionality was observed between the moduli of crosslinked substrates and the number-average molecular weight of V-PDMS, confirming the role of this end-functionalized pre-polymer as the backbone of the network.

Meanwhile, substrate modulus dropped with decreasing density of -SiH moieties on PHMS, reflecting the impact of the decreasing average number of backbones attached per crosslinker (<n>). In addition, while the tunability of substrate moduli as a function of 1) the molecular weight of the backbone and 2) the -SiH density on the crosslinker is still limited by the commercial availability of different types of pre-polymers, the varying ratio between mutually reactive functional groups on the crosslinker and the backbone pre-polymers ([-SiH]:[Vinyl]) proves to be a more versatile parameter in manipulating substrate moduli. The distinct impacts of the increasing [-SiH]:[Vinyl] on substrates prepared with PHMS-991 and PHMS-301 reflect the composite effects of an increasing crosslinker concentration and a decreasing <n>; the distinction also reveals the relative effectiveness of the two types of crosslinkers. Also, the robustness of PHMS-991 as effective crosslinker even with significantly low <n> suggests that, given a constant molecular weight of backbone, substrate modulus is not determined by <n> alone; the distribution of all possible n values of a crosslinker also plays a role.

For future work, the established relations between substrate moduli and pre-polymer formulations will be used to generate cell migration fields with stiffness gradient via photo-initiated hydrosilylation. The specific geometry of interest consists of one lower modulus stripe with adjustable width on a higher modulus field. Efforts will be focused on fine-tuning the width of the soft stripe and the steepness of the modulus gradient, which are shown to be major factors

affecting mechanotaxis behaviors. Also, proper model for AFM measurement should be developed to characterize moduli of specified domains.

*Surface PEGylation.* PEGylation on PDMS surfaces first requires activation of the inert surfaces with functional groups. In this project, introducing -SiH functionality during the preparation of crosslinked PDMS effectively eliminates this additional activation step. Relative surface density of -SiH can be readily controlled with [-SiH]:[Vinyl] ratio during the preparation of crosslinked PDMS thin films. An improved hydrophilic character of PEGylated surfaces was observed with increasing surface density of -SiH. The hydrophilic character was further enhanced with a lower curing temperature (90°C) of PDMS thin films, which effectively preserved surface -SiH from oxidative consumptions. However, high advancing contact angles and surface hysteresis constantly observed after PEGylation are most likely due to the chemical heterogeneity of surfaces, indicating insufficient PEG coverage. Efforts were therefore devoted to increasing PEG coverage via 1) developing better -SiH preservation strategies, 2) increasing the molecular weight of grafted PEG, and 3) pinpointing the ideal catalyst concentration for effective PEGylation.

$O_2$ depravation during the preparation of PDMS thin films proves to be a non-ideal strategy to conserve -SiH, due to the role of $O_2$ as a co-catalyst during hydrosilylation. PEGylation using PEG with higher molecular weight did not significantly decrease the advancing contact angles. Fine-tuning PEGylation on PHMS monolayers, on the other hand, revealed the impact of catalyst

concentration on PEGylation efficiency and helped pinpoint the ideal catalyst concentration (67 ppm, by weight of Pt) for effective PEGylation.

Possible future directions can be divided into two main categories. First, the selected catalyst concentration for effective PEGylaiton on PHMS monolayers will be translated onto crosslinked PDMS thin films. If this improved condition did not reduce the high advancing contact angles as it did on PHMS surfaces, the most probable reason would be an insufficient -SiH surface density on the crosslinked PDMS surfaces. In that case, strategies should be developed to increase -SiH surface density. Second, it is important to better understand the impact of PEG molecular weight on PEGylation efficiency. A lowest possible molecular weight will be searched such that sufficient coverage of grafted PEG does not change established substrate moduli. This part of the project will depend on AFM characterizations for both the surface topography and the moduli of crosslinked PDMS thin films.

**References:**


1. Klaus von der, M.; Jung, P.; Sebastian, B.; Patrik, S. *Cell Tissue Res*. **2010**, 339, 131–153.
2. Carter, S. B. *Nature.* **1965**, 208, 1183–1187.
3. Harris, A. K. *Exp. Cell Res.* **1973**, 77, 285–297.
4. Pettit, E. J.; Fay, F. S. *Physiol. Rev.* **1998**, 78, 949–967.
5. Lo, C.; Wang, H.; Dembo, M.; Wang, Y. *Biophysical Journal* **2000**, 79 (1), 144–152.
6. Song, S.; Kim, M.; Shin, J. H. *Conf Proc IEEE Eng Med Biol Soc* **2009**, 2106-10.
7. Kawano, T.; Kidoaki, S. *Biomaterials* **2011**, 32 (11), 2725-2733.
8. Gray, D. S.; Tien, J.; Chen, C. S. *J Biomed Mater Res* **2003**, 66 (3), 605-14.
9. Wong, J. Y.; Velasco, A.; Rajagopalan, P.; Pham, Q. *Langmuir* **2003**, 19 (5), 1908–1913.
10. Burdick, J. A.; Khademhosseini, A.; Langer, R. *Langmuir* **2004**, *20* (13), 5153–5156.
11. Zaari, N.; Rajagopalam, P.; Kim, S. K.; Engler, A. J.; Wong, J. Y. *Adv Mater* **2004**,16, 23-24.
12. Isenberg, B. C.; Dimilla, P. A.; Walker, M.; Kim, S.; Wong, J. Y. *Biophys J*, **2009**, 97 (5), 1313-1322.
13. Cheung, Y. K.; Azeloglu, E. U.; Shiovitz, D. A.; Costa, K. D.; Seliktar, D.; Sia, S. K. *Angew. Chem. Int. Ed.* **2009**, 48, 7188 –7192
14. Hadjipanayi, E.; Mudera, V.; Brown, R. A. *Cell Motility Cytoskeleton* **2009**, 66 (3), 121-8.
15. Hale, N. A.; Yang, Y.; Rajagopalan, P. *ACS Appl Mater Interfaces* **2010**, 2(8), 2317-24.
16. Hahn, M. S.; Miller, J. S.; West, J. L. *Adv Mater* **2006**, 18 (20), 2679–2684.
17. Nemir, S.; Hayenga, H. N.; West, J. L. *Biotechnol. Bioeng*. **2009**, 105 (3), 636-44.
18. Kidoaki, S.; Matsuda,T. *J Biotechnol* **2008**, 133 (2), 225-30.
19. Geiger, B.; Bershadsky, A.; Pankov, R.; Yamada, K. M. *Nat. Rev. Mol. Cell Biol.* **2001,** 2(11), 793-805.
20. Williams, D. F. *The Williams Dictionary of Biomaterials*. Liverpool University Press: Liverpool, **1999**.
21. Engler, A. J.; Sen, S.; Sweeney, H. L.; Discher, D. E. *Cell* **2006**, 126, 677-689.
22. Gibbs, G. V.; Hamil, M. M.; Louisnathan, S. J., *American Mineralogist* **1972**, 57, 1578-1613.
*23.* Thomas, X., *Inorganic Polymers.* Nova Science Publishers: U.K.
*24.* Lehmann, R. G. *Degradation in Silicone Polymers in Nature;* Midland, MI, 1998.
25. Nicholson, J. W., *Polymer.* Royal Society of Chemistry: Great Britain, **2006**.

26. Rochow, E. G., *An Introduction to the Chemistry of the Silicones*. J. Wiley & Sons Chapman & Hall: New York London, **1946**.
27. Wright, J. G. E.; Oliver, C. S., U.S.Patent 2,448,565, September 7, **1948**.
28. Marsden, J., U.S. Patent 2,445,794, July 27, **1948**.
29. Marciniec, B. *Hydrosilylation: Advances in Silicon Science*; Springer, **2009**.
30. Karstedt, B. D. U.S. Patent 3,775,452, Nov. 27, **1973**.
31. Lewis, L. N. *J. Am. Chem. SOC*. **1990,** 112, 5998.
32. Zhixin Wang. PhD. Dissertation, University of South Florida, 2011.
33. Mechanical Testing and Properties of Plastics: An Introduction*, ASM Hand Book*; ASM International, 2003; pp 26-41.
34. Frantz, C; Stewart, K. M.; Weaver, V. M. *Journal of Cell Science* 123, 4195-4200
35. Anderson, J. M.; Rodriguez, A.; Chang, D. T. *Seminars in Immunology* **2008**, 20, 86–100.
36. Hillborg, H.; Tomczak, N.; Olah, A.; Schonherr, H.; Vancso, G. J. *Langmuir* **2004**, 20 (3), 785-794.
37. Wang, B.; Abdulali-Kanji, Z.; Dodwell, E.; Horton, J. H.; Oleschuk, R. D. *Electrophoresis* **2003**, 24 (9), 1442-1450.
38. Hu, S. W.; Ren, X. Q.; Bachman, M.; Sims, C. E.; Li, G. P.; Allbritton, N. *Anal. Chem.* **2002**, 74 (16), 4117-4123.
39. Thermo Scientific. Protein Methods Library: Polyethylene Glycol (PEG) and Pegylation of Proteins. http://www.piercenet.com (accessed Apr 16, 2013).
40. Chen, H.; Brook, M. A.; Sheardown, H. *Biomaterials* **2004,** 25, 2273.
41. Kingshott, P.; Griesser, and H. J. *Curr. Opin. Solid State Mater. Sci.* **1999,** 4, 403.
42. Morra, M. *J. Biomater. Sci. Polymer Edn.* **2000,** 11, 547.
43. Unsworth, L. D.; Sheardown, H.; Brash, J. L. *Langmuir* **2005,** 21, 1036.
44. Bailon, P.; Won, C. Y. *Expert Opin. Drug Deliv.* **2009,** 6, 1.
45. Ryan, S. M.; Mantovani, G.; Wang, X. X.; Haddleton, D. M.; Brayden, D. M. *Expert Opin. Drug Deliv.* **2008,** 5, 371.
46. Szleifer, I. *Curr. Opin. Colloid Interf. Sci.* **1996,** 1, 416.
47. Szleifer, I. Biophys. J. **1997,** 72, 595.
48. Szleifer, I. Physica A **1997,** 244, 370.
49. Szleifer, I. Curr. Opin. Solid State Mater. Sci. **1997,** 2, 337.
50. Antonsen, K. P.; Hoffman, A. S Water structure of PEG solutions by differential scanning calorimetry measurements. In *Poly(Ethylene Glycol) Chemistry: Biotechnical and Biomedical Applications;* Harris, J.M., Ed.; Plenum Press: New York, 1992; pp 15–28.
51. Gombotz, W.; Guanghui, W.; Horbett, T.; Hoffman, A. Protein adsorption to and elution from polyether surfaces. In *Poly(Ethylene Glycol) Chemistry: Biotechnical and Biomedical Applications; Harris, J.M., Ed.;* Plenum Press, New York, 1992; pp 247–260.
52. Halperin, A. *Langmuir* **1999,** 15, 2525-2533.

53. Heuberger, M.; Drobek, T.; Spencer, N. D. *Biophysical Journal* **2005,** 88, 495–504.
54. B. J. Klenkler and H. Sheardown, *Biotechnol. Bioeng.* **2006,** 95, 1158.
55. Wei, S. Q.; Bai, Y. P.; Shao, L. *Eur. Polym. J.* **2008,** 44, 2728.
56. Bodas, D.; Rauch, J. Y.; Khan-Malek, C. *Eur. Polym. J.* **2008,** 44, 2130.
57. Ren, T. B.; Weigel, T.; Groth, T.; Lendlein, A. *J. Biomed. Mater. Res. A* **2008,** 86, 209.
58. Chen, H.; Brook, M. A.; Sheardown, H. *Biomaterials,* **2004***,* 25, 2273-2282.
59. Mikhail, A. S.; Ranger, J. J.; Liu, L; Longenecker, R.; Thompsonb, D. B.; Sheardowna, H. D.; Brook, M. A. *J. Biomater. Sci.* **2010,** 21, 821-842.
60. Wenzel, R .N. *J. Phys. Chem.* **1949,** 53 (9), 1466–1467.
61. Gray, D. S.; Tien, J.; Chen, C. S. J. *Biomed Mater Res A.* **2003,** 66 (3), 605-614.
62. Meyers, K. O.; Bye, M. L.; Merrill, E. W. *Macromolecules* **1980,** 13, 1045.
63. Mark, J. E. "Elastomers and Rubber Elasticity", Chap.18.
64. Bye, M. L. M. S. Thesis in Chem. Eng., M.I.T. 1980.
65. Meyers, K. O.; Merrill, E. W. "Elastomers and Rubber Elasticity", Chap 17.
66. Niwano, M.; Kageyama, J.; Kurita, K., Kinashi, K.; Takahashi, I.; Miyamoto, N. *J. Appl. Phys.* **1994,** 76 (4), 2157-2163.
67. Mark, J. E.; Sullivan, J. L., *J. Chem. Phys*. **1977,** 66, 1006.
68. Mark, J. E., *Makromol. Chem. Suppl.* **1979,** 2, 87.
69. Sung, P. H.; Mark, J. E., *Eur. Polym. J.* **1980,** 16, 1223.
70. Sung, P. H.; Mark, J. E., *J. Polym. Sci., Polym. Phys. Ed.* **1981,** 19, 507.
71. Sung, P, H.; Pan, S. J.; Mark, J. E.; Chang, V. S. C.; Lackey, J. E.; Kennedy, J. P., *Polym. Bull.* **1983,** 9, 375.
72. Queslel, J.P.; Mark, J. E., *Adv. Polym. Sci.* **1984,** 65, 137-157.
73. Larsen, A. L.; Larsen, P. S.; Hassager, O. *e-Polymers* **2004,** no. 050.
74. Langley, N. R. *Macromolecules* **1968,** 1, 348.
75. Dossin, L. M.; Graessley, W. W. *Macromolecules* **1969,** 12, 123.
76. Wikipedia. http://en.wikipedia.org/wiki/Thin_film (accessed April 15, 2013)
77. Luengo, L.; Schmitt, F. J.; Hill, R.; Israelachvili, J. *Macromolecules* **1997,** 30 (8), pp 2482–2494.
78. Macleod, H. A. *Journal of Vacuum Science & Technology A: Vacuum, Surfaces, and Films 4.3* **1986,** pp 418-422.
79. Johnson, K. L.; Kendall, K.; Roberts, A. D. *Proc. R. Soc*. **1971,** 324, 301-313.
80. Xu, W.; Chahine, N.; Sulchek, T. *Langmuir* **2011,** 27, 8470–8477.
81. Sen, S.; Engler, A. J.; Discher, D. E. *Cell Mol Bioeng* **2009,** 2, 39–48.
82. Buxboim, A.; Rajagopal, K.; Brown, A. E. X.; Discher, D. E. *J Phys Condens Matter* **2010,** 22, 1–10.
83. Zaslavsky, B. Y.; Baevskii, A. V.; Rogozhin, S. V.; Gedrovich, A. V.; Shishkov, A. V.; Gasanov, A. A.; Masimov, A. A. *Journal of Chromatography A* **1984,** 285, 63-68.
84. Backmann, N.; Kappeler, N.; Braun, T.; Huber, F.; Lang, H.; Gerber, C.; Roderick, Y. H. *Beilstein J. Nanotechnol.* **2010,** 1, 3-13.